CHAPTER 11

GEOTECHNICAL DESIGN OF DRILLED SHAFTS UNDER AXIAL LOADING

11.1 INTRODUCTION

The methods used to analyze and design drilled shafts under axial loading have evolved since the 1960s, when drilled shafts came into wide use. The design methods recommended for use today reflect the evolution of construction practices developed since that time.

11.2 PRESENTATION OF THE FHWA DESIGN PROCEDURE

11.2.1 Introduction

This chapter presents methods for computation of the capacity of drilled shafts under axial loading. The methods for computation of axial capacity were developed by O'Neill and Reese (1999).

The methods of analysis assume that excellent construction procedures have been employed. It is further assume that the excavation remained stable, and was completed with the proper dimensions, that the rebar was placed properly, that a high-slump concrete was used, that the concrete was placed in a correct manner, that the concrete was placed within 4 hours of the time that the excavation was completed, and that any slurry that was used was properly conditioned before the concrete was placed. Much additional information on construction methods is given in O'Neill and Reese (1999). Another FHWA publication (LCPC, 1986), translated from French, also gives much useful information.

While the design methods presented here have proved to be useful, they are not perfect. Research continues on the performance of drilled shafts, and improved methods for design are expected in the future. An appropriate factor of safety must be employed to determine a safe working load. The engineer may elect to employ a factor of safety that will lead to a conservative assessment of capacity if the job is small. A load test to develop design parameters or to prove the design is strongly recommended for a job of any significance.

11.3 STRENGTH AND SERVICEABILITY REQUIREMENTS

11.3.1 General Requirements

Two methods are available for determining the factored moments, shears, and thrusts for designing structures by the strength design method: the single-load factor method and a method based on the American Concrete Institute Building Code (ACI 318).

In addition to satisfying strength and serviceability requirements, many structures must satisfy stability requirements under various loading and foundation conditions.

11.3.2 Stability Analysis

The stability analysis of structures such as retaining walls must be performed using unfactored loads. The unfactored loads and the resulting reactions are then used to determine the unfactored moments, shears, and thrusts at critical sections of the structure. The unfactored moments, shears, and thrusts are then multiplied by the appropriate load factors, and the hydraulic load factor when appropriate, to determine the required strengths used to establish the required section properties.

The single-load factor method must be used when the loads on the structural component being analyzed include reactions from a soil–structure interaction stability analysis, such as footings for walls. For simplicity and ease of application, this method should generally be used for all elements of such structures. The load factor method based on the ACI 318 Building Code may be used for some elements of the structure, but must be used with caution to ensure that the load combinations do not produce unconservative results.

11.3.3 Strength Requirements

Strength requirements are based on loads resulting from dead and live loads, hydraulic loading, and seismic loading.

11.4 DESIGN CRITERIA

11.4.1 Applicability and Deviations

The design criteria for drilled shafts generally follow the recommendations for structures founded on driven piles for loading conditions and design factors of safety.

11.4.2 Loading Conditions

Loading conditions are generally divided into cases of usual, unusual, and extreme conditions.

11.4.3 Allowable Stresses

No current design standard contains limitations on allowable stresses in concrete or steel used in drilled shafts. However, the recommendations of ACI 318-02, Section A.3 may be used as a guide for design. These recommendations are summarized in Table 11.1.

In cases where a drilled shaft is fully embedded in clays, silts, or sands, the structural capacity of the drilled shaft is usually limited by the allowable moment capacity. In the case of drilled shafts socketed into rock, the structural capacity of the drilled shaft may be limited by the allowable stress in the shaft. Maximum shear force usually occurs below the top of rock.

11.5 GENERAL COMPUTATIONS FOR AXIAL CAPACITY OF INDIVIDUAL DRILLED SHAFTS

The axial capacity of drilled shafts should be computed by engineers who are thoroughly familiar with the limitations of construction methods, any special requirements for design, and the soil conditions at the site.

TABLE 11.1 Permissible Service Load Stresses Recommended by ACI 318-95, Section A.3

Case	Stress Level*
Flexure—extreme fiber stress in compression	$0.45\ f'_c$
Shear—shear carried by concrete	$1.1\sqrt{f'_c}$
Shear—maximum shear carried by concrete plus shear reinforcement	$v_c + 4.4\sqrt{f'_c}$
Tensile stress—Grade 40 or 50 reinforcement	20,000 psi
Tensile stress—Grade 60 reinforcement	24,000 psi

*v_c = permissible shear stress carried by concrete, psi, f'_c = compressive strength of concrete, psi.

The axial capacity of a drilled shaft may be computed by the following formulas:

$$Q_{\text{ult}} = Q_s + Q_b \tag{11.1}$$

$$Q_s = f_s A_s \tag{11.2}$$

$$Q_b = q_{\max} A_b \tag{11.3}$$

where

Q_{ult} = axial capacity of the drilled shaft,
Q_s = axial capacity in skin friction,
Q_b = axial capacity in end bearing,
f_s = average unit side resistance,
A_s = surface area of the shaft in contact with the soil along the side of the shaft,
$q_{\max}$ = unit end-bearing capacity, and
A_b = area of the base of the shaft in contact with the soil.

11.6 DESIGN EQUATIONS FOR AXIAL CAPACITY IN COMPRESSION AND IN UPLIFT

11.6.1 Description of Soil and Rock for Axial Capacity Computations

The following six subsections present the design equations for axial capacity in compression and in uplift. The first five subsections present the design equations in side resistance and end bearing for clay, sand, clay shales, gravels, and rock. The last section presents a discussion of a statistical study of the performance of the design equations in clays and sands.

O'Neill and Reese (1999) introduced the descriptive terms used in this book to describe soil and rock for axial capacity computations. Collectively, all types of soil and rock are described as *geomaterials.* The basic distinction between soil and rock types is the characteristic of cohesiveness. All soil and rock types include the descriptive terms *cohesive* or *cohesionless.*

11.6.2 Design for Axial Capacity in Cohesive Soils

Side Resistance in Cohesive Soils The basic method used for computing the unit load transfer in side resistance (i.e., in skin friction) for drilled shafts in cohesive soils is the *alpha* (α) *method.* The profile of undrained shear strength c_u of the clay versus depth is found from unconsolidated-undrained

triaxial tests, and the following equation is employed to compute the ultimate value of unit load transfer at a depth z below the ground surface:

$$f_s = \alpha\, c_u \tag{11.4}$$

where

f_s = ultimate load transfer in side resistance at depth z,
c_u = undrained shear strength at depth z, and
α = empirical factor that can vary with the magnitude of undrained shear strength, which varies with depth z.

The value of α includes the effects of sampling disturbance on the soil's shear strength, migration of water from the fluid concrete into the soil, and other factors that might affect axial capacity in side resistance.

The total load Q_s in side resistance is computed by multiplying the unit side resistance by the peripheral area of the shaft. This quantity is expressed by

$$Q_s = \int_{z_{\text{top}}}^{z_{\text{bot}}} f_{sz}\, dA \tag{11.5}$$

where

dA = differential area of perimeter along sides of drilled shaft over penetration depth,
L = penetration of drilled shaft below ground surface,
z_{top} = depth to top of zone considered for side resistance, and
z_{bot} = depth to bottom of zone considered for side resistance.

The peripheral areas over which side resistance in clay is computed are shown in Figure 11.1. The upper portion of the shaft is excluded for both compression and uplift to account for soil shrinkage in the zone of seasonal moisture change. In areas where the depth of seasonal moisture change is greater than 5 ft (1.5 m) or when substantial groundline deflection results from lateral loading, the upper exclusion zone should be extended to deeper depths. The lower portion of the shaft is excluded when the shaft is loaded in compression because downward movement of the base will generate tensile stresses in the soil that will be relieved by cracking of soil, and porewater suction will be relieved by inward movement of groundwater. If a shaft is loaded in uplift, the exclusion of the lower zone for straight-sided shafts should not be used because these effects do not occur during uplift loading.

The value of α is the same for loading in both compression and uplift.

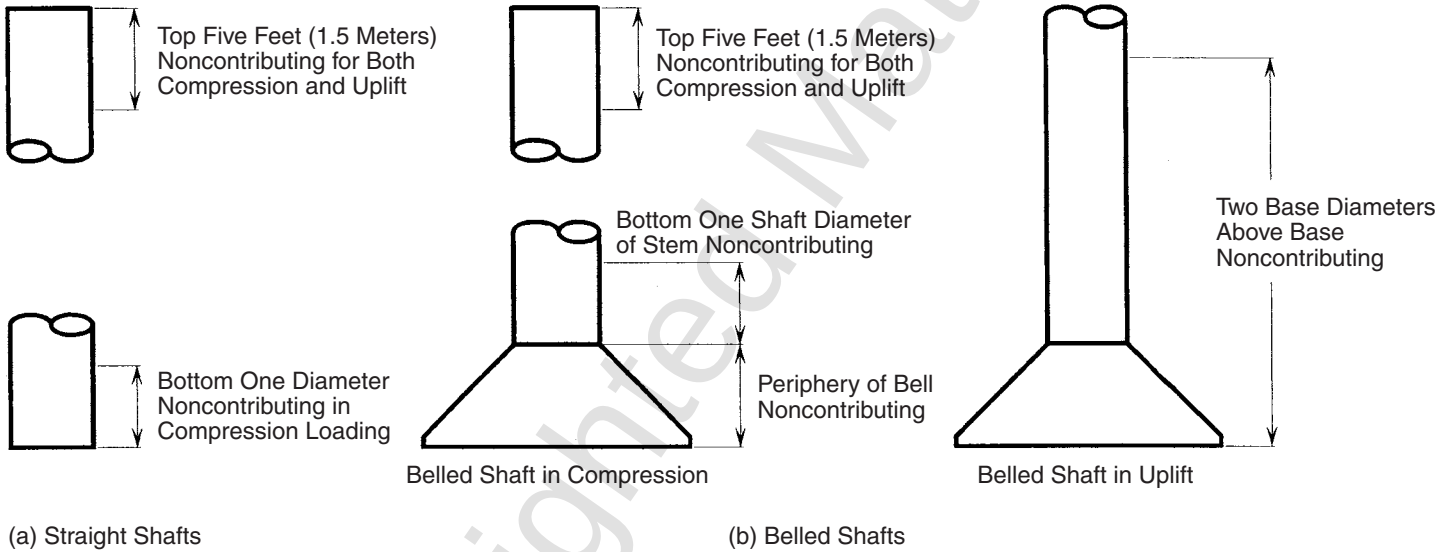

Figure 11.1 Portions of drilled shaft not considered in computing side resistance in clay.

If the shaft is constructed with an enlarged base (also called an *underream* or a *bell*), the exclusion zones for side resistance at the bottom of the shaft differ for loading in compression and uplift, as shown in Figure 11.1b. If the shaft is loaded in compression, the lower exclusion zone includes the upper surface of the bell and the lower one diameter of the shaft above the bell. When a belled shaft is loaded in uplift, the lower exclusion zone for side resistance extends two base diameters above the base. If the lower exclusion zone overlaps the upper exclusion zone, then no side resistance is considered in the computations of axial capacity in uplift.

Equation 11.4 indicates that the unit load transfer in side resistance at depth z is a product of α and undrained shear strength at depth z. Research on the results of load tests of instrumented drilled shafts has found that α is not a constant and that it varies with the magnitude of the undrained shear strength of cohesive soils. O'Neill and Reese (1999) recommend using

$$\alpha = 0.55 \quad \text{for} \quad \frac{c_u}{p_a} \leq 1.5 \tag{11.6a}$$

and

$$\alpha = 0.55 - 0.1\left(\frac{c_u}{p_a} - 1.5\right) \quad \text{for} \quad 1.5 \leq \frac{c_u}{p_a} \leq 2.5 \tag{11.6b}$$

where p_a = atmospheric pressure = 101.3 kPa = 2116 psf. (Note that 1.5 p_a = 152 kPa or 3,170 psf and 2.5 p_a = 253 kPa or 5290 psf.)

For cases where c_u/p_a exceeds 2.5, side resistance should be computed using the methods for cohesive intermediate geomaterials, discussed later in this chapter.

Some experimental measurements of α obtained from load tests are shown in Figure 11.2. The relationship for α as a function of c_u/p_a defined by Eq. 11.6 is also shown in this figure. For values of c_u/p_a greater than 2.5, side resistance should be computed using the recommendations for cohesive intermediate geomaterials, discussed later in this chapter.

When an excavation is open prior to the placement of concrete, the lateral effective stresses at the sides of the drilled hole are zero if the excavation is drilled in the dry or small if there is drilling fluid in the excavation. Lateral stresses will then be imposed on the sides of the excavation because of the fluid pressure of the fresh concrete. At the ground surface, the lateral stresses from the concrete will be zero or close to zero. It can be expected that the lateral stress from the concrete will increase almost linearly with depth, assuming that the concrete has a relatively high slump. Experiments conducted by Bernal and Reese (1983) found that the assumption of a linear increase in the lateral stress from fluid concrete for depths of concrete of 3.0 m (10 ft) or more is correct. For depths greater than 3.0 m, the lateral stress is strongly

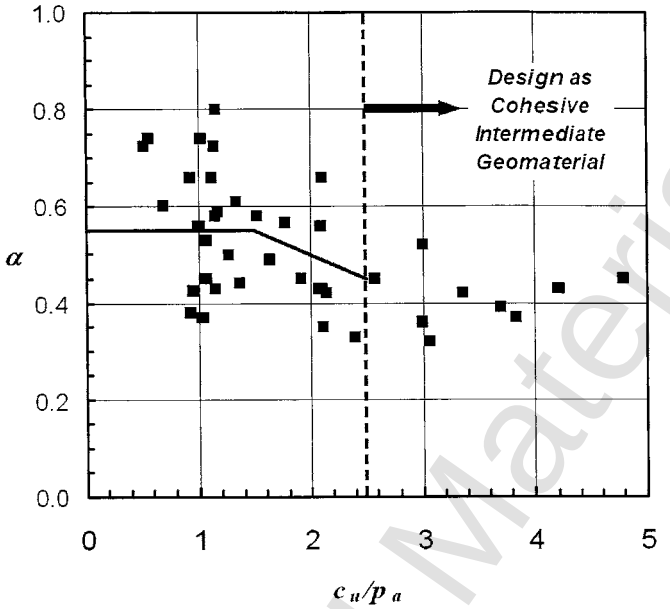

Figure 11.2 Correlation between α and c_u/p_a.

dependent on the character of the fresh concrete. From available experimental evidence, it follows that a rational recommendation for α is that α should vary perhaps linearly with depth, starting at zero at the groundline, to its ultimate value at some critical depth below the groundline. However, insufficient data are available for making such a detailed recommendation. The recommendations for design in Eq. 11.6 generally lead to a reasonable correlation between experimental measurements and computed results.

With regard to the depth over which α is assumed to be zero, consideration must be given to those cases where there are seasonal changes in the moisture content of the soil. It is conceivable, perhaps likely, that clay near the ground surface will shrink away from the drilled shaft so that the load transfer is reduced to zero in dry weather over the full depth of the seasonal moisture change. There may also be other instances where the engineer may wish to deviate from the recommendations of Eq. 11.6 because of special circumstances at a particular site. A drilled shaft subjected to a large lateral load is an example of such a circumstance; if the lateral deflection at the groundline is enough to open a gap between the shaft and soil, the portion of the drilled shaft above the first point of zero deflection should be excluded from side resistance.

End Bearing in Cohesive Soils The computation of load transfer in end bearing for deep foundations in clays is subject to much less uncertainty than

is the computation of load transfer in side resistance. Skempton (1951) and other investigators have developed consistent formulas for the computation of end bearing. In addition, the accuracy of Skempton's work has been confirmed by results from instrumented drilled shafts where general base failure was observed. Equation 11.7 is employed for computing the ultimate unit end bearing $q_{\max}$ for drilled shafts in saturated clay:

$$q_{\max} = N_c^* c_u \tag{11.7}$$

where c_u is an average undrained shear strength of the clay computed over a depth of two diameters below the base, but judgment must be used if the shear strength varies strongly with depth.

The bearing capacity factor N_c^* is computed using

$$N_c^* = 1.33(\ln|I_r| + 1) \tag{11.8}$$

where I_r is the rigidity index of the soil, which for a saturated, undrained material ($\phi = 0$) soil is expressed by

$$I_r = \frac{E_s}{3c_u} \tag{11.9}$$

where E_s is Young's modulus of the soil undrained loading. E_s should be measured in laboratory triaxial tests or in-situ by pressuremeter tests to apply the above equations. For cases in which measurements of E_s are not available, I_r can be estimated by interpolation using Table 11.2.

When L/B is less than 3.0, $q_{\max}$ should be reduced to account for the effect of the presence of the ground surface by using

$$q_{\max} = 0.667\left[1 + 0.1667\,\frac{L}{B}\right] N_c^* c_u \tag{11.10}$$

where:

TABLE 11.2 I_r and N_c^* Values for Cohesive Soil

c_u	I_r	N_c^*
24 kPa (500 psf)	50	6.55
48 kPa (1000 psf)	150	8.01
96 kPa (2000 psf)	250	8.69
192 kPa (4000 psf)	300	8.94

L = length of the shaft, and
B = diameter of the base of the shaft.

Uplift Resistance of Straight-Sided Shafts in Cohesive Soil Base resistance for uplift loading on straight-sided shafts should be assumed to be zero unless confirmed by load testing.

Uplift Resistance of Belled Shafts in Cohesive Soil Unit base resistance for belled shafts can be computed from

$$q_{\max}\ (\text{uplift}) = s_u N_u \tag{11.11}$$

where

N_u = bearing capacity factor for uplift, and
s_u = average undrained shear strength between the base of the bell and 2 B_b above the base.

N_u can be computed from

$$N_u = 3.5\,\frac{D_b}{B_b} \le 9 \quad \text{for unfissured clay} \tag{11.12}$$

or from

$$N_u = 0.7\,\frac{D_b}{B_b} \le 9 \quad \text{for fissured clay} \tag{11.13}$$

In the expressions above, D_b is the depth of the base of the bell below the top of the soil stratum that contains the bell, but not counting any depth within the zone of seasonal moisture change.

The unit uplift resistance should be applied over the projected area of the bell, A_u. The projected area is computed from

$$A_u = \frac{\pi}{4}\,(B_b^2 - B^2) \tag{11.14}$$

Example Problem 1—Shaft in Cohesive Soil This is an example of a shaft drilled into clay. It is based on a case history, referred to as ''Pile A,'' reported by Whitaker and Cooke (1966).

Soil Profile. The soil profile is shown in Figure 11.3. The clay is overconsolidated. The depth to the water table was not given and is not needed in making capacity calculations. However, the range of depth of the water table

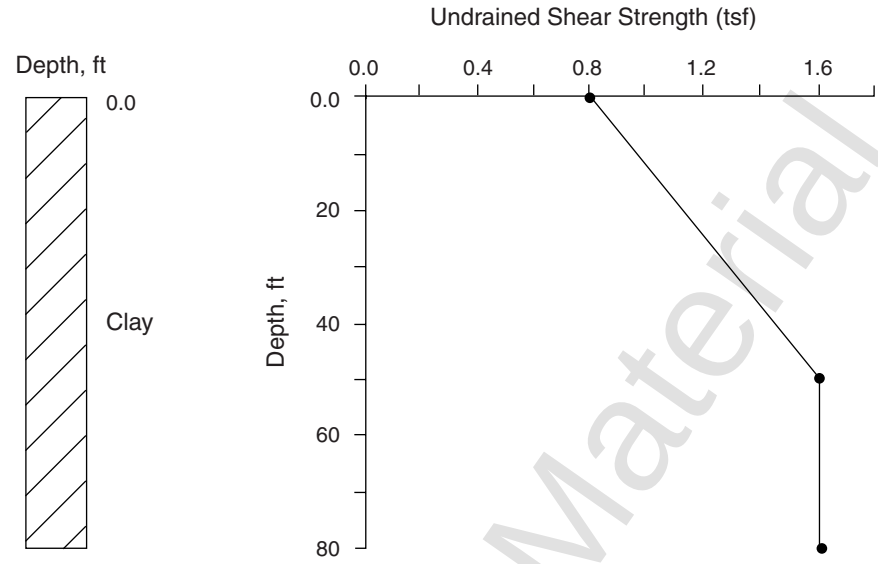

Figure 11.3 General soil description of Example Problem 1.

should be determined and always reported in the construction documents for construction considerations.

Soil Properties. Values of undrained shear strength obtained from laboratory tests are included in Figure 11.3.

Construction. High-quality construction, good specifications, and excellent inspection are assumed.

Loadings. The working axial load is 230 tons. No downdrag acting on the shaft is expected, and vertical movement of the soil due to expansive clay is not a problem. Effects due to lateral loading are also thought to be negligible. The depth to the zone of seasonal moisture change is judged to be about 10 ft.

Factor of Safety. It is assumed that a load test has been performed in the area, that the design parameters have been proven, and that the soil conditions across the site are relatively uniform; therefore, an overall factor of safety of 2 was selected.

Ultimate Load. Using a factor of safety of 2, the ultimate axial load was computed to be 460 tons.

Geometry of the Drilled Shaft. An underreamed shaft was designed to penetrate a total of 40 ft into the clay. The height of the bell is 4 ft, making the

length of the straight-sided portion 36 ft. The diameter of the straight-sided portion of the shaft is 2.58 ft, and the diameter of the bell is 5.5 ft.

Computations

SIDE RESISTANCE. For ease of hand computations, a constant value of α_z equal to 0.55 and an average c_u of 2280 psf are assumed. However, the computer program interpolates linearly the top and bottom values of c_u with depth. The hand computations are as follows:

Depth Interval, ft	ΔA, ft^2	Avg. Effective Stress, tsf	α_Z	ΔQ_s, tons
0–5			0	0
5–33.4	230.4	1.14	0.55	144.4
33.4–40			0	0
				Q_s = 144.4

BASE RESISTANCE. The average undrained shear strength over two base diameters below the base is 1.48 tsf, and the area of the base is 23.76 ft^2.

By interpolation between the values of N_c^* shown in Table 11.2, N_c^* = 8.81.

$q_{\max} = N_c^* c_u$ = (8.81) (1.48 tsf) = 13.04 tsf
A_b = 23.76 ft^2
Q_b = (12.92 tsf) (23.76 ft^2) = 309.8 tons

TOTAL RESISTANCE

Q_T = 144.3 + 307 = 454 tons

11.6.3 Design for Axial Capacity in Cohesionless Soils

Side Resistance in Cohesionless Soils The shear strength of sands and other cohesionless soils is characterized by an angle of internal friction that ranges from about 30° up, depending on the kinds of grains and their packing. The cohesion of such soils is assumed to be zero. The friction angle at the interface between the concrete and the soil may be different from that of the soil itself. The unit side resistance, as the drilled shaft is pushed downward, is equal to the normal effective stress at the interface times the tangent of the interface friction angle.

Unsupported shaft excavations are prone to collapse, so excavations in cohesionless soil are made using drilling slurry to stabilize the borehole, and the normal stress at the face of the completed drilled shaft depends on the construction method. The fluid stress from the fresh concrete will impose a

normal stress that is dependent on the characteristics of the concrete. Experiments have found that concrete with a moderate slump (up to 6 in., 150 mm) acts hydrostatically over a depth of 10 to 15 ft (3 to 4.6 m) and that there is a leveling off in the lateral stress at greater depths, probably due to arching (Bernal and Reese, 1983). Concrete with a high slump (about 9 in., 230 mm) acts hydrostatically to a depth of 32 ft (10 m) or more. Thus, the construction procedures and the nature of the concrete will have a strong influence on the magnitude of the lateral stress at the concrete–soil interface. Furthermore, the angle of internal friction of the soil near the interface will be affected by the details of construction.

In view of the above discussion, the method of computing the unit load transfer in side resistance must depend on the results from field experiments as well as on theory. The following equations are recommended for design. The form of the equations is based on theory, but the values of the parameters that are suggested for design are based principally on the results of field experiments.

$$f_{sz} = K\sigma'_z \tan \phi_c \tag{11.15}$$

$$Q_s = \int_0^L K\sigma'_z \tan \phi_c \, dA \tag{11.16}$$

where

f_{sz} = ultimate unit side resistance in sand at depth z,
K = a parameter that combines the lateral pressure coefficient and a correlation factor,
σ'_z = vertical effective stress in soil at depth z,
ϕ_c = friction angle at the interface of concrete and soil,
L = depth of embedment of the drilled shaft, and
dA = differential area of the perimeter along sides of drilled shaft over the penetration depth.

Equations 11.15 and 11.16 can be used in the computations of side resistance in sand, but simpler expressions can be developed if the terms for K and tan ϕ_c are combined. The resulting expressions are shown in Eqs. 11.17 through 11.20.

$$f_{sz} = \beta \, \sigma'_z \leq 2.1 \text{ tsf} \quad (200 \text{ kPa}) \tag{11.17}$$

$$Q_s = \int_0^L \beta\sigma'_z \, dA \tag{11.18}$$

$$\beta = 1.5 - 0.135\sqrt{z\ (\text{ft})} \quad \text{or}$$
$$\beta = 1.5 - 0.245\sqrt{z\ (\text{m})}; \quad 0.25 \le \beta \le 1.20 \tag{11.19a}$$

where z = depth below the ground surface, in feet or meters, as indicated.

When the uncorrected SPT resistance, N_{60}, is less than or equal to 15 blows/ft, β is computed using

$$\beta = \frac{N_{60}}{15}\left(1.5 - 0.135\sqrt{z\ (\text{ft})}\right) \quad \text{or}$$
$$\beta = \frac{N_{60}}{15}\left(1.5 - .245\sqrt{z\ (\text{m})}\right) \quad \text{for } N_{60} \le 15 \tag{11.19b}$$

Note that for sands

$$\beta = 0.25 \quad \text{when} \quad z > 85.73 \text{ ft or } 26.14 \text{ m} \tag{11.20}$$

For very gravelly sands or gravels

$$\beta = 2.0 - 0.0615\ [z\ (\text{ft})]^{0.75} \quad \text{or}$$
$$\beta = 2.0 - 0.15\ [z\ (\text{m})]^{0.75}; \quad 0.25 \le \beta \le 1.8 \tag{11.21}$$

For gravelly sands or gravels

$$\beta = 0.25 \quad \text{when} \quad z > 86.61 \text{ ft} \quad \text{or} \quad 26.46 \text{ m} \tag{11.22}$$

The design equations for drilled shafts in sand use SPT N_{60}-values uncorrected for overburden stress. The majority of the load tests on which the design equations are based were performed in the Texas Gulf Coast region and the Los Angeles Basin in California. The N_{60}-values for these load tests were obtained using donut hammers with a rope-and-pulley hammer release system. If a designer has N-values that were measured with other systems or were corrected for level of overburden stress and rod energy, it will be necessary to adjust the corrected N-values to the uncorrected N_{60} form for donut hammers with rope-and-pulley hammer release systems before use in the design expressions of Eq. 11.19b and Table 11.4. Guidance for methods used to correct SPT penetration resistances is presented in Chapter 3 of EM 1110-1-1905.

The parameter β combines the influence of the coefficient of lateral earth pressure and the tangent of the friction angle. The parameter also takes into account the fact that the stress at the interface due to the fluid pressure of the concrete may be greater than that from the soil itself. In connection with the

lateral stress at the interface of the soil and the concrete, the assumption implicit in Eq. 11.17 is that good construction procedures are employed. See Chapter 5 for further construction information. Among other factors, the slump of the concrete should be 6 in. or more and drilling slurry, if employed, should not cause a weak layer of bentonite to develop at the wall of the excavation. The reader is referred to O'Neill and Reese (1999) for further details on methods of construction.

The limiting value of side resistance shown in Eq. 11.17 is not a theoretical limit but is the largest value that has been measured (Owens and Reese, 1982). Use of higher values can be justified by results from a load test.

A comparison of β values computed from Eq. 11.19 and β values derived from loading tests in sand on fully instrumented drilled shafts is presented in Figure 11.4. As can be seen, the recommended expression for β yields values that are in reasonable agreement with experimental values.

Equation 11.17 has been employed in computations of f_{sz}, and the results are shown in Figure 11.5. Three values of β were selected; two of these are in the range of values of β for submerged sand, and the third is an approximate value of β for dry sand. The curves are cut off at a depth below 60 ft (18 m) because only a small amount of data has been gathered from instrumented drilled shafts in sand with deep penetrations. Field load tests are indicated if drilled shafts in sand are to be built with penetrations of over 70 ft (21 m).

It can be argued that Eqs. 11.17 and 11.18 are too elementary and that the angle of internal friction, for example, should be treated explicitly. However, the drilling process has an influence on in situ shearing properties, so the true friction angle at the interface cannot be determined from a field investigation that was conducted before the shaft was constructed. Furthermore, Eqs. 11.17 and 11.18 appear to yield an satisfactory correlation with results from full-scale load tests.

The comparisons of results from computations with those from experiments, using the above equations for sand, show that virtually every computed value is conservative (i.e., the computed capacity is less than the experimentally measured capacity). However, it is of interest that most of the tests in sand are at locations where the sand was somewhat cemented. Therefore, caution should be observed in using the design equations for sand if the sand is clean, loose, and uncemented.

Either Eq. 11.15 or Eq. 11.17 can be used to compute the side resistance in sand. The angle of internal friction of the sand is generally used in Eq. 11.15 in place of the friction angle interface at the interface of the concrete and soil if no information is available. In some cases, only SPT resistance data are available. In such cases, the engineer can convert the SPT penetration resistance to the equivalent internal friction angle by using Table 11.3 as a guide.

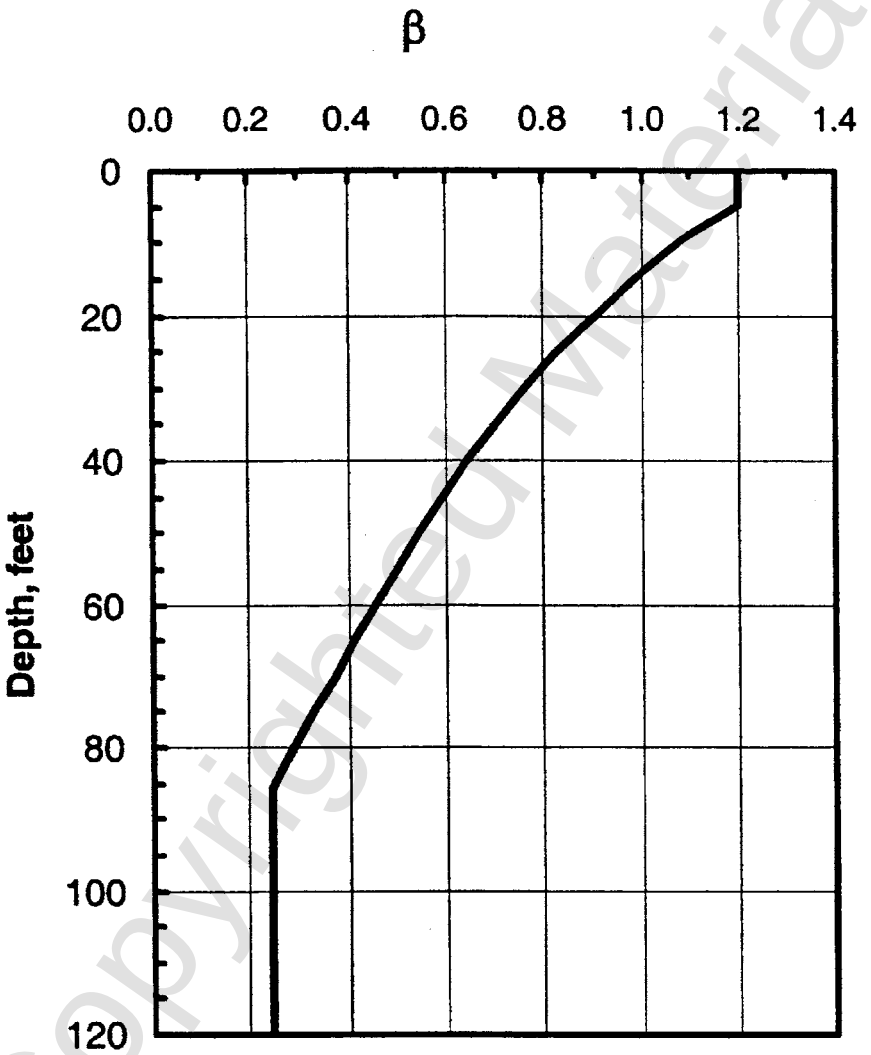

Figure 11.4 Plot of experimental values of β.

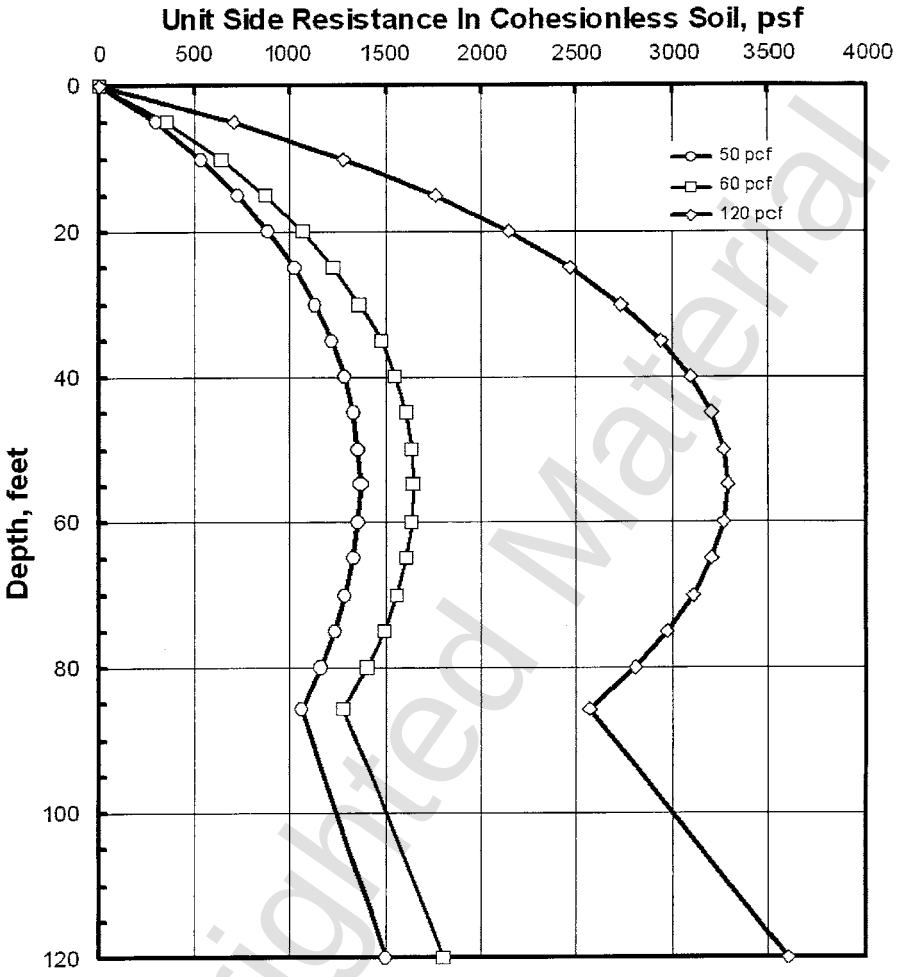

Figure 11.5 Variation of f_{sz} with depth (z) for values of γ.

Side Resistance in Cohesionless Soils—Uplift Loading For uplift loading in granular materials, the side resistance developed under drained, uplift conditions is reduced due to the Poisson effect, lowering the normal stress at the side of the shaft. Based on analytical modeling and centrifuge research reported by de Nicola (1996), side resistance in uplift may be computed using

$$f_{\max}\ (\text{uplift}) = \Psi\ f_{\max}\ (\text{compression}) \tag{11.23}$$

The factor Ψ is computed using

TABLE 11.3 Relationship Between N, ϕ, and D_r

N	ϕ, deg.	D_r, %	ϕ, deg.	D_r, %	ϕ, deg.	D_r, %
2	32	45				
4	34	55				
6	36	65	30	37		
10	38	75	32	46	31	40
15	42	90	34	57	32	48
20	45	100	36	65	34	55
25			37	72	35	60
30			39	77	36	65
35			40	82	36	67
40			41	86	37	72
45			42	90	38	75
50			44	95	39	77
55			45	100	39	80
60					40	83
65					41	86
70					42	90
75					42	92
80					43	95
85					44	97
90					44	99

Source: After Gibbs and Holtz (1957).

$$\eta = v_p \tan \delta \left(\frac{L}{B}\right)\left(\frac{G_{\text{avg}}}{E_p}\right) \tag{11.24}$$

$$\Psi = \left\{1 - 0.2 \log_{10}\left|\frac{100}{(L/B)}\right|\right\}(1 - 8\eta + 25\eta^2) \tag{11.25}$$

where

E_p = Young's modulus of the shaft, and
G_{avg} = average shear modulus of the soil along the length of the shaft, estimated as the average Young's modulus of soil divided by 2.6.

O'Neill and Reese (1999) examined Eq. 11.25 and concluded that typical values of Ψ fall into the range 0.74 to 0.85 for L/B ratios of 5 to 20. They noted that Eq. 11.25 appears to overestimate Ψ for L/B ratios larger than 20. The value Ψ can be taken conservatively to be 0.75 for design purposes.

End Bearing in Cohesionless Soils Because of the relief of stress when an excavation is drilled into sand, the sand tends to loosen slightly at the

bottom of the excavation. Also, there appears to be some densification of the sand beneath the base of a drilled shaft as settlement occurs. A similar phenomenon has also been observed in model tests on spread footings founded in sand by Vesić (1973). The load-settlement curves for the base of drilled shafts that have been obtained from load tests on instrumented test shafts are consistent with these concepts. In many load tests, the base load continued to increase to a settlement of more that 15% of the diameter of the base. Such a large settlement cannot be tolerated for most structures; therefore, it was decided to formulate the design equations for end bearing to limit values of end bearing for drilled shafts in granular soil to those that are expected to occur at a downward movement of 5% of the diameter of the base (O'Neill and Reese, 1999).

Values of q_b are tabulated as a function of N_{60} (standardized for hammer energy but uncorrected for overburden stress) in Table 11.4. The computation of tip capacity is based directly on the penetration resistance from the SPT near the tip of the drilled shaft.

The values in Table 11.4 can be expressed in equation form as follows:

$$\text{If } L \geq 10 \text{ m:} \quad q_b = 57.5\, N_{\text{SPT}} \leq 2.9 \text{ MPa} \tag{11.26}$$

$$\text{If } L < 10 \text{ m:} \quad q_b = \frac{L}{10 \text{ m}}\, 57.5\, N_{SPT} \leq \frac{L}{10 \text{ m}}\, 2.9 \text{ MPa} \tag{11.27}$$

or in U.S. Customary Units

$$\text{If } L \geq 32.8 \text{ ft:} \quad q_b = 0.60\, N_{SPT} \leq 30 \text{ tsf} \tag{11.28}$$

$$\text{If } L < 32.8 \text{ ft:} \quad q_b = \frac{L}{32.8 \text{ ft}}\, 0.60\, N_{SPT} \leq \frac{L}{32.8 \text{ ft}}\, 30 \text{ tsf} \tag{11.29}$$

where L is the shaft length in meters or feet as required.

These values are similar to those recommended by Quiros and Reese (1977). These authors recommended no unit end bearing for loose sand

TABLE 11.4 Recommended Values of Unit End Bearing for Shafts in Cohesionless Soils with Settlements Less Than 5% of the Base Diameter

Range of Value on N_{60}	Value of q_b, tons/ft^2	Value of q_b, MPa
0 to 50 blows/ft	0.60 N_{60}	0.0575 N_{60}
Upper limit	30 tsf	2.9 MPa

Note: For shafts with penetrations of less than 10 base diameters, it is recommended that q_b be varied linearly from zero at the groundline to the value computed at 10 diameters using Table 11.4.

($\phi \leq 30°$), a value of 16 tons/ft^2 (1.53 MPa) for medium-dense sand ($30° < \phi \leq 36°$), and a value of 40 tons/ft^2 (3.83 MPa) for very dense sand ($36° < \phi \leq 41°$).

Neither of the sets of recommendations involves the stress in the soil outside the tip of the drilled shaft. This concept is consistent with the work of Meyerhof (1976) and others. Furthermore, the values in Table 11.4 are based predominantly on experimental results for shaft settlements of less than 5% of the base diameter where the drilled shafts had various penetrations. However, implicit in the values of q_b that are given is that the penetration of the drilled shaft must be at least 10 diameters below the ground surface. For penetration of less than 10 diameters, it is recommended that q_b be varied linearly from zero at the groundline to the value computed at 10 diameters using Table 11.4.

Table 11.4 sets the limiting value of load transfer in end bearing at 30 tsf (2.9 MPa) at a settlement equal to 5% of the base diameter. However, higher unit end-bearing values are routinely used when validated by load tests. For example, a value of 58 tsf (5.6 MPa) was measured at a settlement of 4% of the diameter of the base at a site in Florida (Owens and Reese, 1982).

Example Problem 2—Shaft in Cohesionless Soil This is an example of a shaft drilled into sand. The example has been studied in the referenced literature of Reese and O'Neill (1988). It is also modeled after load tests in sand (Owens and Reese, 1982).

Soil Profile. The soil profile is shown in Figure 11.6. The water table is at a depth of 4 ft below the ground surface.

Soil Properties. N_{60}-values (blow counts per foot) from the SPT are included in Figure 11.6.

Construction. High-quality construction is assumed. The contractor will have all the required equipment in good order, and experienced personnel will be on the job.

Loadings. The working axial load is 170 tons, the lateral load is negligible, and no downdrag is expected.

Factor of Safety. It is assumed that a load test has been performed nearby, but considering the possible variation in the soil properties over the site and other factors, an overall factor of safety of 2.5 is selected. The diameter will be sufficiently small so that reduced end bearing will not be required. Consequently, the global factor of safety can be applied to both components of resistance.

Ultimate Load. The ultimate axial load is thus established as 2.5×170 tons $= 425$ tons, since a global factor of safety (of 2.5) is used.

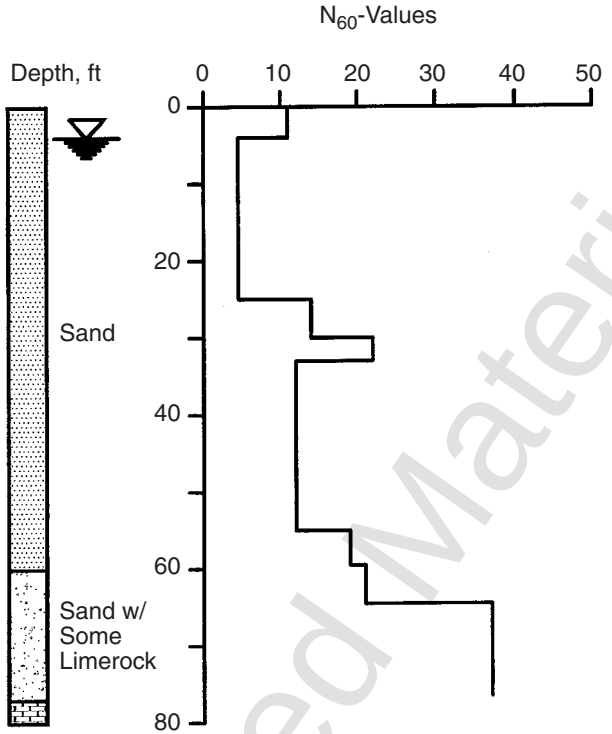

Figure 11.6 General soil description of Example Problem 2.

Geometry of the Drilled Shaft. A straight-sided drilled shaft is selected with a diameter of 3 ft and a penetration of 60 ft.

Computations

SIDE RESISTANCE. Computations are performed assuming a total unit weight of sand equal to 115 pcf. The hand computations are as follows:

Depths, ft	ΔA, ft^2	Avg. Effective Stress, tsf	β	ΔQ_s, tons
0–4	37.7	0.115	1.200	5.2
4–30	245.0	0.572	0.943	132.1
30–60	282.7	1.308	0.594	219.7
				Q_s = 357.0 tons

BASE RESISTANCE. Computations for base resistance are performed using the soil at the base of the shaft. At the 60-ft location, N_{SPT} = 21.

$$q_b = 0.60N_{SPT} \leq 30 \text{ tsf}$$
$$q_b = (0.6)\ (21) = 12.6 \text{ tsf}$$

$A_b = 7.07 \text{ ft}^2$
$Q_b = (7.07 \text{ ft}^2)\ (12.6 \text{ tsf}) = 89.1 \text{ tons}$

TOTAL RESISTANCE

$Q_T = 357 + 89.1 = 446.1 \text{ tons}$

Example Problem 3—Shaft in Mixed Profile This is an example of a shaft drilled into a soil of a mixed profile with layers of clay and sand. It is modeled after load tests performed and reported by Touma and Reese (1972) at the G1 site.

Soil Profile. The soil profile is shown in Figure 11.7. The water table is at a depth of 17 ft below the ground surface.

Soil Properties. Values of undrained shear strength obtained from laboratory tests and N_{60}-values (blow counts per foot) from the SPT are included in Figure 11.7.

Construction. High-quality construction, good specifications, and excellent inspection are assumed.

Loadings. The working axial load is 150 tons, no downdrag is expected, and lateral loading is negligible. The depth to the zone of seasonal moisture change is judged to be about 10 ft.

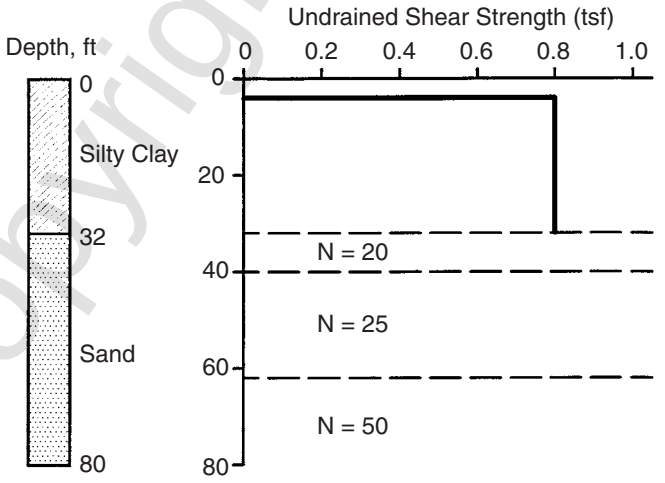

Figure 11.7 General soil description of Example Problem 3.

Factor of Safety. Soil conditions across the site are variable, and the foundation is for a major and complex structure. An overall factor of safety of 3 was selected.

Ultimate Load. Using the factor of safety of 3, the ultimate axial load is computed to be 450 tons.

Geometry of the Drilled Shaft. A straight-sided shaft is selected, with a diameter of 3 ft and a penetration of 59 ft.

Computations

SIDE RESISTANCE. Computations are performed assuming a total unit weight of clay equal to 125 pcf and a total unit weight of sand equal to 115 pcf. For ease of hand computations, an average value of β was selected for the sand layer. The computations are as follows:

Soil Type	Depth Interval, ft	ΔA, ft^2	Avg. c_u or Effective Stress, tsf	α_Z or β	ΔQ_s, tons
Clay	0–5	—	(Cased)	0	0
Clay	5–32	254.5	0.81	0.55	113.4
Sand	32–59	254.5	1.887	0.589	282.9
					Q_s = 396.3 tons

BASE RESISTANCE. Computations for base resistance are performed using the soil at the base of the shaft. At the 59-ft location, N_{SPT} = 25.

q_b = (0.6) (25 tsf) = 15.0 tsf
A_b = 7.07 ft^2
Q_b = (7.07 ft^2) (15.0 tsf) = 106.0 tons

TOTAL RESISTANCE

Q_T = 396.3 + 106.0 = 502.3 tons

11.6.4 Design for Axial Capacity in Cohesive Intermediate Geomaterials and Jointed Rock

Side Resistance in Cohesive Intermediate Geomaterials *Weak rock* is the term for materials that some authors call *intermediate geomaterials.* In general, the soil resistances and settlements computed by these criteria are considered appropriate for weak rock with compressive strength in the range

of 0.5 to 5.0 MPa (73 to 725 psi). The following intermediate geomaterials usually fall within this category: argillaceous geomaterials (such as heavily overconsolidated clay, hard-cohesive soil, and weak rock such as claystones) or calcareous rock (limestone and limerock, within the specified values of compressive strength).

Drilled shafts are attractive as a reliable foundation system for use in intermediate geomaterials. These geomaterials are not difficult to excavate, and provide good stability and excellent capacity.

Two procedures for computation of side resistance in cohesive intermediate geomaterials are presented by O'Neill and Reese (1999). One procedure is a simplified version of a more detailed procedure developed by O'Neill et al. (1996). Both procedures are presented in the following sections.

Simplified Procedure for Side Resistance in Cohesive Intermediate Geomaterial. The first decision to be made by the designer is whether to classify the borehole as smooth or rough. A borehole can be classified as rough only if artificial means are used to roughen its sides and to remove any smeared material from its sides. If conditions are otherwise, the borehole must be classified as smooth for purposes of design.

The term *smooth* refers to a condition in which the borehole is cut naturally with the drilling tool without leaving smeared material on the sides of the borehole wall. To be classified as rough, a borehole must have keys cut into its wall that are at least 76 mm (3 in.) high, 51 mm (2 in.) deep, and spaced vertically every 0.46 m (1.5 ft) along the depth of shafts that are at least 0.61 m (24 in.) in diameter.

The peak side resistance for a smooth borehole in Layer i is computed using

$$f_{\max,i} = \alpha\varphi q_{u,i} \tag{11.30}$$

where α (not equal in value to the α for cohesive soils) is obtained from Figure 11.8. The terms in the figure are defined as follows. E_m is Young's modulus of the rock (i.e., the rock mass modulus), q_u is the unconfined strength of the intact material, and w_t is the settlement at the top of the rock socket at which α is developed. The rock mass modulus can be estimated from measurements of Young's modulus of intact rock cores using Table 11.6. The curves in Figure 11.8 are based on the assumption that the interface friction angle between the rock and concrete is 30°. If the interface friction is different from 30°, it should be modified using

$$\alpha = \alpha_{\phi_{rc}=30^\circ} \frac{\tan\phi_{rc}}{\tan 30^\circ} \tag{11.31}$$

or

$$\alpha = 1.73\alpha_{\phi_{rc}=30^\circ} \tan \phi_{rc}$$

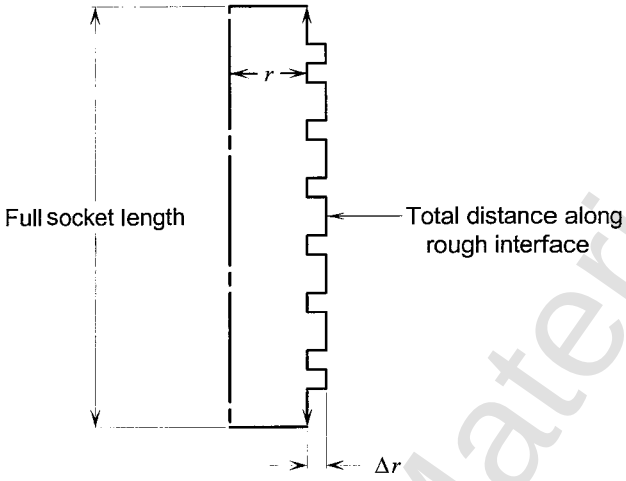

Figure 11.8 Definition of terms for surface roughness.

To use Figure 11.8, the designer must estimate the horizontal pressure of the fluid concrete acting at the middle of Layer i, σ_n. If the concrete has a slump of 175 mm (7 in.) or more and is placed at a rate of 12 m (40 ft) per hour, then σ_n at a depth z_i^* below the cutoff elevation up to 12 m (40 ft) can be estimated from

$$\sigma_n = 0.65\gamma_c z_i^* \tag{11.32}$$

φ is a joint effect factor that accounts for the presence of open joints that are voided or filled with soft gouge material. The joint effect factor can be estimated from Table 11.5.

$q_{u,i}$ is the design value for q_u in Layer i. This is usually taken as the mean value from intact cores larger than 50 mm (2 in.) in diameter. The possibility of the presence of weaker material between the intact geomaterial that could be sampled is considered through the joint effect factor, φ.

For a smooth rock socket in cohesive intermediate geomaterial, the side resistance is computed using

TABLE 11.5 Estimation of E_m/E_i Based on RQD

RQD (%)	Closed Joints	Open Joints
100	1.00	0.60
70	0.70	0.10
50	0.15	0.10
20	0.05	0.05

$$f_{\max,i} = 0.65\varphi\, p_a \sqrt{\frac{q_{u,i}}{p_a}} \tag{11.33}$$

If the rock socket has been roughened, the side resistance for a rough rock socket in cohesive intermediate geomaterial is

$$f_{\max,i} = 0.8\varphi \left(\frac{\Delta r}{r} \left(\frac{L'}{L} \right) \right]^{0.45} q_{u,i} \tag{11.34}$$

where

Δr = depth of shear keys,
r = radius of borehole,
L' = vertical spacing between the shear keys, and
L = depth covered by the shear keys, as defined in Fig. 11.9.

Detailed Procedure for Side Resistance in Cohesive Intermediate Geomaterial. O'Neill et al. (1996) recommend methods for estimating side and base resistances as well as settlement of drilled shafts under axial loads in this type of geomaterial. Their primary method, called *direct load-settlement sim-*

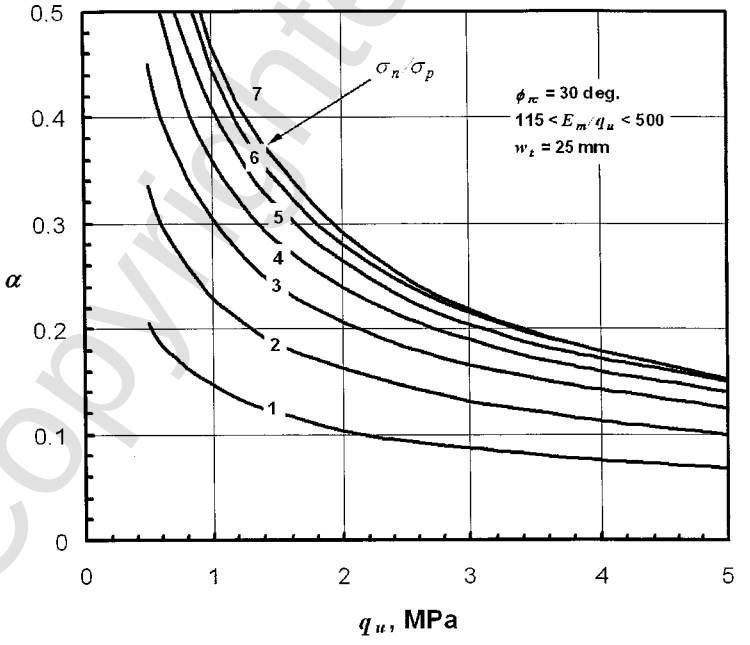

Figure 11.9 Factor α for smooth category 1 or 2 IGMs.

ulation, is used to compute the axial capacity of drilled shafts socketed into weak rock.

The direct simulation design model, based on an approximation of the broad range of FEM solutions, is as follows:

Decide whether the socket of weak rock in which the drilled shaft is placed requires subdivision into sublayers for analysis. If the weak rock is relatively uniform, the behavior of axially loaded drilled shafts can probably be simulated satisfactorily for design purposes using the simple procedure outlined below. If there is significant layering of the weak rock in the depth range of the socket, a load transfer function analysis should be modeled by a special FEM, as recommended by O'Neill et al. (1996). Significant layering in this respect will exist if the weak rock at the base of the shaft is considerably stronger and stiffer than that surrounding the sides and/or if changes in the stiffness and strength of the weak rock occur along the sides of the shaft. Load transfer function analyses should also be conducted if sockets exceed about 7.6 m (25 ft) in length.

Obtain representative values of the compressive strength q_c of the weak rock. It is recognized in practice that q_u is often used to represent compressive strength. Accordingly, q_u will be used to symbolize q_c in this criteria. Whenever possible, the weak rock cores should be consolidated to the mean effective stress in the ground and then subjected to undrained loading to establish the value of q_u. This solution is valid for soft rocks with $0.5 < q_u < 5.0$ MPa ($73 < q_u < 725$ psi). The method also assumes that high-quality samples, such as those obtained using triple-walled core barrels, have been recovered.

Determine the percentage of core recovery. If core recovery using high-quality sampling techniques is less than 50%, this method does not apply, and field loading tests are recommended to establish the design parameters.

Determine or estimate the mass modulus of elasticity of the weak rock, E_m. If Young's modulus of the material in the softer seams within the harder weak rock, E_s, can be estimated, and if Young's modulus of the recovered, intact core material, E_i, is measured or estimated, then the following expression, can be used:

$$\frac{E_m}{E_i} = \frac{L_c}{\dfrac{e_i}{E_s}\sum t_{\text{seams}} + \sum t_{\text{intact core segments}}} \tag{11.35}$$

In Eq. 11.32, L_c is the length of the core and Σt_{seams} is the summation of the thickness of all of the seams in the core, which can be assumed to be $(1 - r_c)\, L_c$, where r_c is the core recovery ratio (percent recovery/100%) and can be assumed equal to $r_c\, L_c$. If the weak rock is uniform and without significant soft seams or voids, it is usually conservative to take $E_m = 115\, q_u$. If the core recovery is less than 100%, it is recommended that appropriate in situ tests be conducted to determine E_m. If the core recovery is at least

50%, the recovered weak rock is generally uniform and the seams are filled with soft geomaterial, such as clay, but moduli of the seam material cannot be determined. Table 11.6 can be used, with linear interpolation if necessary, to estimate very approximately E_m/E_i. Use of this table is not recommended unless it is impossible to secure better data.

The designer must decide whether the walls in the socket can be classified as rough. If experience indicates that the excavation will produce a borehole that is rough according to the following definition, then the drilled shaft may be designed according to the method for the rough borehole. If not, or if the designer cannot predict the roughness, the drilled shaft should be designed according to the method for the smooth borehole.

A borehole can be considered rough if the roughness factor R_f will reliably exceed 0.15. The roughness factor is defined by

$$R_f = \left[\frac{\Delta r}{r}\left(\frac{L_t}{L_s}\right)\right] \tag{11.36}$$

where the terms in this equation are defined in Figure 11.9.

Estimate whether the soft rock is likely to smear when drilled with the construction equipment that is expected on the job site. *Smear* in this sense refers to the softening of the wall of the borehole due to drilling disturbance and/or exposure of the borehole to free water. If the thickness of the smear zone is expected to exceed about 0.1 times the mean asperity height, the drilled shaft should be designed as if it were smooth.

The effects of roughness and smear on both resistance and settlement are very significant, as will be demonstrated in the design examples. As part of the site exploration process for major projects, full-sized drilled shaft excavations should be made so that the engineer can quantify these factors, either by entering the borehole or by using appropriate down-hole testing tools such as calipers and sidewall probes. Rough borehole conditions can be assured if the sides of the borehole are artificially roughened by cutting devices on the drilling tools immediately prior to placing concrete such that $R_f > 0.15$ is attained.

Estimate f_a, the apparent maximum average unit side shear at infinite displacement. Note that f_a is not equal to $f_{\max}$, which is defined as a displacement defined by the user of this method.

TABLE 11.6 Estimation of E_m/E_i Based on RQD

RQD (%)	Closed Joints	Open Joints
100	1.00	0.60
70	0.70	0.10
50	0.15	0.10
20	0.05	0.05

For weak rock with a rough borehole, use

$$f_a = \frac{q_u}{2} \tag{11.37}$$

For weak rock with a smooth borehole, use

$$f_a = \alpha\, q_u \quad \text{where} \quad \alpha \leq 0.5 \tag{11.38}$$

where α is a constant of proportionality that is determined from Figure 11.9 based on the finite element simulations. The factor σ_p in Figure 11.9 is the value of atmospheric pressure in the units employed by the designer. The maximum value of α that is permitted is 0.5. The parameter ϕ_{rc} in Figure 11.9 represents the angle of internal friction at the interface of the weak rock and concrete. The curves of Figure 11.9 are based on the use of $\phi_{rc} = 30°$, a value measured at a test site in clay-shale that is believed to be typical of clay-shales and mudstones in the United States. If evidence indicates that ϕ_{rc} differs from 30°, then α should be adjusted using Eq. 11.39:

$$\alpha = \alpha_{\text{Figure 11.8}} \frac{\tan \phi_{rc}}{\tan 30°} = 1.73\, (\alpha_{\text{Figure 11.8}}) \tan \phi_{rc} \tag{11.39}$$

If $E_m/E_i < 1$, adjust f_a for the presence of soft geomaterial within the soft rock matrix using Table 11.7. Define the adjusted value of f_a as f_{aa}. E_m can be estimated from the E_m/E_i ratios based on RQD of the cores. In cases where RQD is less than 50%, it is advisable to make direct measurements of E_m in situ using plate loading tests, borehole jacks, large-scale pressuremeter test, or by back-calculating E_m from field load tests of drilled shafts. The correlations shown in Table 11.7 become less accurate with decreasing values of RQD.

Estimate σ_n, the normal stress between the concrete and borehole wall at the time of loading. This stress is evaluated when the concrete is fluid. If no other information is available, general guidance on the selection of σ_n can be

TABLE 11.7 Adjustment of f_a for the Presence of Soft Seams

E_m/E_i	f_{aa}/f_a
1	1.0
0.5	0.8
0.3	0.7
0.1	0.55
0.05	0.45
0.02	0.3

obtained from Eq. 11.40, which is based on measurements made by Bernal and Reese (1983):

$$\sigma_n = M\ \gamma_c z_c \tag{11.40}$$

where

γ_c = unit weight of the concrete,
z_c = distance from the top of the completed column of concrete to the point in the borehole at which σ_n is desired, usually the middle of the socket, and
M = an empirical factor which depends upon the fluidity of the concrete, as indexed by the concrete slump (obtained from Figure 11.10).

The values shown in Fig. 11.10 represent the distance from the top of the completed column of concrete to the point in the borehole at which σ_n is desired. Figure 11.10 may be assumed valid if the rate of placement of concrete in the borehole exceeds 12 m/hr and if the ratio of the maximum coarse aggregate size to the borehole diameter is less than 0.02. Note that σ_n for slump outside the range of 125 to 225 mm (5 to 9 in.) is not evaluated. Unless there is information to support larger values of σ_n, the maximum value of z_c should be taken as 12 m (40 ft) in these calculations. This statement is predicated on the assumption that arching and partial setting will become significant after the concrete has been placed in the borehole for more than 1 hour.

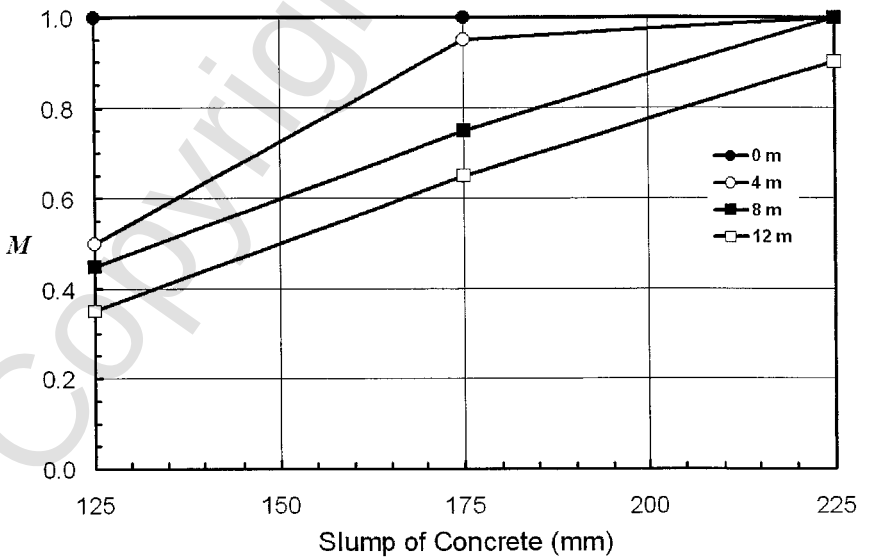

Figure 11.10 Factor M versus slump of concrete.

Note that E_m increases with increasing q_u, and the Poisson effect in the shaft causes an increase in the lateral normal interface stresses as E_m increases, producing higher values of side load transfer at the frictional interface.

Determine the *characteristic parameter n*, which is a fitting factor for the load-settlement syntheses produced by the finite element analyses. If the weak rock socket is rough:

$$n = \frac{\sigma_n}{q_u} \tag{11.41}$$

If the weak rock socket is smooth, estimate n from Figure 11.11. Note that n was determined in Figure 11.11 for $\phi_{rc} = 30°$. It is not sensitive to the value of ϕ_{rc}. However, α is sensitive to ϕ_{rc}, as indicated in Eq. 11.31.

If the socket has the following conditions—relatively uniform, and the soft rock beneath the base of the socket has a consistency equivalent to that of the soft rock along the sides of the shaft, $2 < L/D < 20$, $D > 0.5$ m, and $10 < E_c/E_m < 500$—then compute the load-settlement relation for the weak rock socket as follows. Under the same general conditions, if the socket is highly stratified and/or if the geomaterial beneath the base of the socket has a consistency considerably different from that along the sides of the socket, use the unit load transfer function version of this method described later.

Compute Q_t (load still in the shaft at the top of the socket) versus w_t (settlement at the top of the socket) from Eq. 11.42 or Eq. 11.43, depending on the value of n. These equations apply to both rough and smooth sockets.

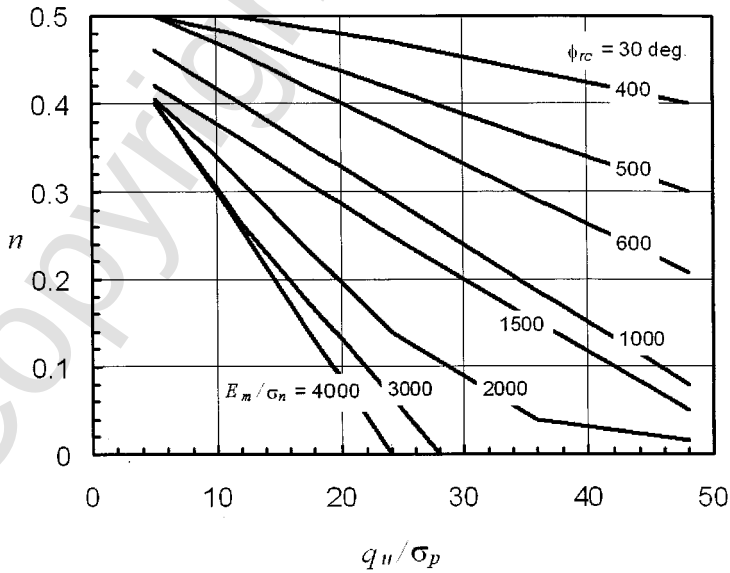

Figure 11.11 Factor n for smooth sockets for various combinations of parameters.

$$\text{If } H_f \le n: \quad Q_t = \pi DLH_f f_{aa} = \frac{\pi D^2}{4} q_b \tag{11.42}$$

$$\text{If } H_f > n: \quad Q_t = \pi DLK_f f_{aa} = \frac{\pi D^2}{4} q_b \tag{11.43}$$

Equation 11.42 applies in the elastic range before any slippage has occurred at the shaft–weak rock interface, and an elastic base response, as represented by the last expression on the right-hand side of the equation, also occurs. Equation 11.43 applies during interface slippage (nonlinear response). To evaluate Q_t, a value of w_t is selected, and H_f, which is a function of w_t, is evaluated before deciding which equation to use. If $H_f > n$, evaluate K_f and use Eq. 11.43; otherwise, use Eq. 11.42. Equations 11.44 and 11.45 are used to evaluate H_f and K_f, respectively.

$$H_f = \frac{E_m \Omega}{\pi L \Gamma f_{aa}} w_t \tag{11.44}$$

$$K_f = n + \frac{(H_f - n)(1 - n)}{H_f - 2n + 1} \le 1 \tag{11.45}$$

where

$$\Omega = 1.14 \left(\frac{L}{D}\right)^{0.5} - 0.05 \left[\left(\frac{L}{D}\right)^{0.5} - 1\right] \log_{10} \left|\frac{E_c}{E_m}\right| - 0.44 \tag{11.46}$$

with $D < 1.53$ m and

$$\Gamma = 0.37 \left(\frac{L}{D}\right)^{0.5} - 0.15 \left[\left(\frac{L}{D}\right)^{0.5} - 1\right] \log_{10} \left|\frac{E_c}{E_m}\right| + 0.13 \tag{11.47}$$

Finally,

$$q_b = \Lambda \, w_t^{0.67} \tag{11.48}$$

where

$$\Lambda = 0.0134 E_m \left(\frac{L/D}{L/D + 1}\right) \left[\frac{200(\sqrt{L/D} - \Omega)(1 + L/D)}{\pi L \Gamma}\right] \tag{11.49}$$

Check the values computed for q_b. If core recovery in the weak rock surrounding the base is 100%, q_b should not exceed $q_{\max} = 2.5 \, q_u$. At working loads, q_b should not exceed $0.4 \, q_{\max}$.

Graph the load-settlement curve resulting from the computations. Select ultimate and service limit resistances based on settlements. For example, the ultimate resistance might be selected as the load Q_t corresponding to a settlement w_t of 25 mm (1 in.), while the service limit resistance might be selected as the load Q_t corresponding to a value of $w_t < 25$ mm ($w_t < 1$ in.).

Example Problem 4—Shaft in Cohesive Intermediate Geomaterial
This is an example of a drilled shaft in weak rock.

Description of the Problem—Rough Socket. Consider the shaft and soil profile shown in Figure 11.12. The user is asked to compute the load-settlement relation for the socket and to estimate the ultimate resistance at a settlement of $w_t = 25$ mm. The socket is assumed to be rough. The RQD for the sample is 100%.

Computations

1. Since the core recovery and RQD are high, assume that $E_m = 115\ q_u$. Note that $E_c/E_m = 100\%$.
2. $f_{aa} = f_a = 2.4/2 = 1.2$ MPa, or 1200 kPa.
3. $z_c = 6.1$ m (depth from the top of the concrete to the middle of the socket). Considering concrete placement specifications:

$$\sigma_n = 0.92\ \gamma_c\ z_c \text{ from Figure 11.12 or}$$

$$\sigma_n = 0.92\ (20.4)\ (6.1) = 114.5 \text{ kPa} = 1.13\ \sigma_p.$$

4. $n = 115$ kPa/2400 kPa $= 0.0477$.
5. $L/D = 6.1/0.61 = 10$.

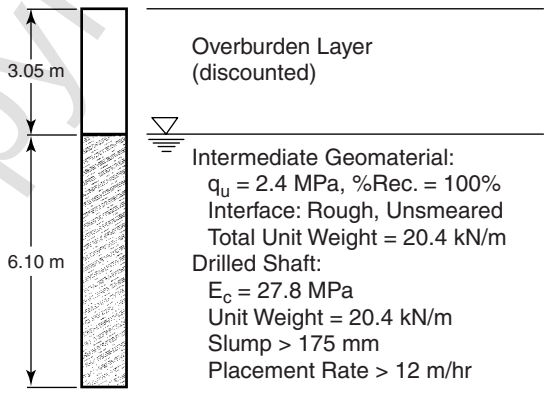

Figure 11.12 General soil description of Example Problem 4.

6. $\Omega = 1.14\sqrt{10} - 0.05\lfloor\sqrt{10} - 1\rfloor\log|100| - 0.44 = 2.949.$
7. $\Gamma = 0.37\sqrt{10} - 0.15\lfloor\sqrt{10} - 1\rfloor\log|100| + 0.13$ or $\Gamma = 0.651.$
8. $H_f = \{[115\ (2400)\ 2.94)]/[3.14\ (6100\ \text{mm})(0.651)\ 1200]\}w_i$

   $H_f = 0.0541\ w_t$
9. $K_f = 0.0477 + (0.0541w_t - 0.0477)\ (1 - 0.0477)/(0.0541w_t - 0.096 + 1)$

   $K_f = 0.0477 + (0.0541w_t - 0.0477)\ (0.952)/(0.0541w_t + 0.904)$
10. At the end of the elastic stage, $\Theta_f = n$ (implied by Eq. 3.44). Therefore,

$$w_{te} = n/\Theta = 0.0477/0.0541 = 0.882\ \text{mm}$$

    where w_{te} signifies w_t at the end of the elastic stage. (Note that the elastic response occurs only up to a very small settlement in this example.)
11. $q_b = \Lambda w_t^{0.67}$ (Eqs. 3.50 and 3.51)

    $q_b = \{[(115)\ (2400)\ (10/11)\}\ \{[200\ (10^{0.5} - 2.949)\ (11)]/[3.14\ (6100)\ 0.651]\}^{0.67}\ w_t^{0.67}$

    $q_b = 373.4\ w_t\ (\text{mm})^{0.67}$ (kPa). Note that $\Lambda = 373.4$.
12. $\pi\ DL = 11.69\ \text{m}^2$; $\pi\ D^2/4 = 0.2922\ \text{m}^2$.
13. Compute Q_t corresponding to w_{te}, signified by Q_{te}:

$$Q_{te} = 11.69\ (0.0541)(0.882)(1200) + (0.2922)(373.4)(0.881)^{0.67}$$

$$Q_{te} = 669 + 100 = 769\ \text{kN (Eq. 3.44).}$$

    Note that at this point, 670 kN is transferred to the weak rock in side resistance and 103 kN is transferred in base resistance. (Q_{te}, w_{te}) is a point on the load-settlement curve, and a straight line can be drawn from ($Q_t = 0$, $w_t = 0$) to this point.
14. Compute the values of Q_t for selected values of w_t on the nonlinear portion of the load-settlement curve. Numerical evaluations are made in the following table.

Rough Socket

w_t, mm	H_f	K_f	Q_s, kN	q_b, kPa	Q_b, kN	Q_t, kN
1	0.0541	0.0540	758.2	373.4	109.1	867.3
2	0.1082	0.1046	1466.9	594.2	173.6	1640.5
3	0.1623	0.1500	2103.7	779.7	227.9	2331.6
4	0.2164	0.1910	2679.1	945.4	276.3	2955.4

5	0.2705	0.2282	3201.5	1097.8	320.8	3522.3
6	0.3245	0.2622	3677.9	1240.5	362.5	4040.5
7	0.3786	0.2933	4114.2	1375.5	402.0	4516.2
8	0.4327	0.3219	4515.2	1504.2	439.6	4954.8
9	0.4868	0.3482	4885.0	1627.7	475.7	5360.7
10	0.5409	0.3726	5227.1	1746.8	510.5	5737.6
11	0.5950	0.3953	5544.5	1861.9	544.1	6088.7
12	0.6491	0.4163	5839.9	1973.7	576.8	6416.7
13	0.7032	0.4359	6115.3	2082.4	608.6	6723.9
14	0.7573	0.4543	6372.9	2188.5	639.6	7012.5
15	0.8114	0.4715	6614.2	2292.0	669.8	7284.0
16	0.8654	0.4877	6840.7	2393.3	699.4	7540.2
17	0.9195	0.5028	7053.9	2492.5	728.4	7782.3
18	0.9736	0.5172	7254.7	2589.8	756.9	8011.6
19	1.0277	0.5307	7444.3	2685.3	784.8	8229.1
20	1.0818	0.5435	7623.6	2779.2	812.2	8435.8
21	1.1359	0.5556	7793.3	2871.6	938.2	8632.5
22	1.1900	0.5670	7954.3	2962.5	865.8	8820.1
23	1.2441	0.5779	8107.2	3052.0	891.9	8999.2
24	1.2982	0.5883	8252.6	3140.3	917.7	9170.4
25	1.3523	0.5982	8391.0	3227.4	943.2	9334.2

Note that

$$q_b \text{ (at } w_t = 25 \text{ mm)} = 3.23 \text{ MPa} = 1.34\, q_u < q_{\max} = 2.5\, q_u$$

which is acceptable for the definition of ultimate resistance. Based on base resistance, the working load should be limited to $q_b = q_u$ or w_t should be limited to about 12 mm at the working load. Note also that the compressive stress in the shaft at $w_t = 15$ mm is 24,900 kPa (7284 kN/cross-sectional area), which may be approaching the structural failure load in the drilled shaft.

15. The numerical values from Steps 13 and 14 are graphed in Figure 11.13. Also shown in the figure is the case with a smooth socket for the same problem. Hand computations for the case of a smooth socket are included in the next section.

    The physical significance of the parameters Q_f and K_f is evident from the numerical solution. Q_f is a constant of proportionality for elastic resistance for side shear, and K_f is a proportionality parameter for actual side shear, including elastic, plastic, and interface slip effects.

Description of the Problem—Smooth Socket. Consider the same example as before (shaft and soil profile shown in Figure 11.12). The rock socket is now assumed to be smooth. Estimate that $\phi_{rc} = 30°$. The user is asked to

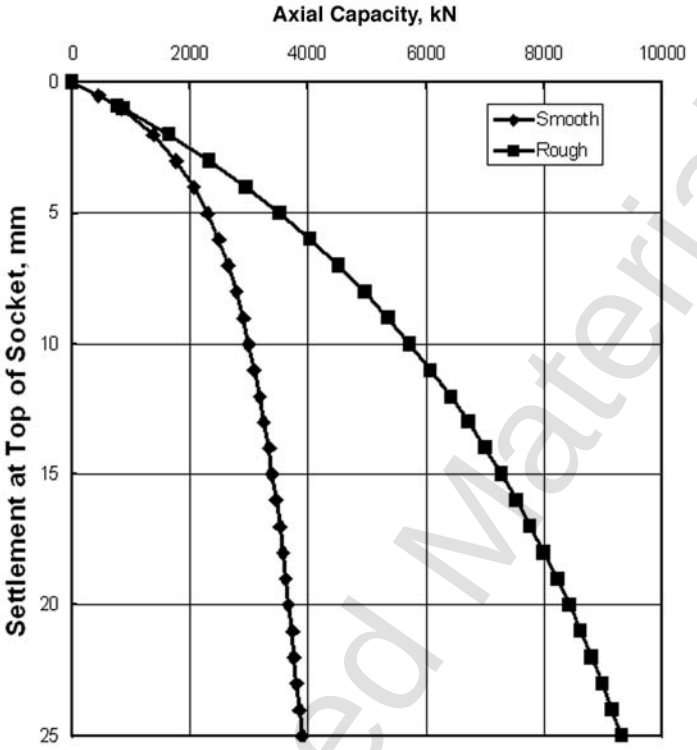

Figure 11.13 Computed axial load versus settlement for Example Problem 4.

compute the load-settlement relation for the socket and to estimate the ultimate resistance at a settlement of $w_t = 25$ mm.

Computations

1. $f_a = f_{aa} = \alpha q_u$.
2. Referring to Figure 11.13, for $\sigma_n/\sigma_p = 1.13$ and $q_u = 2.4$ MPa, we have $\alpha = 0.12$.
3. $f_a = f_{aa} = 0.12(2400) = 288$ kPa.
4. $q_u/\sigma_p = 2400/101.3 = 23.7$ and $E_m/\sigma_n = 115\ (2.4)\ (1000)/114.5 = 2411$.
5. From Figure 11.13, $n = 0.11$.
6. $\Omega = 2.949$ (unchanged); $\Gamma = 0.651$ (unchanged).
7. $H_f = \{[115(2400)\ 2.949)]/[3.14\ (6100\ \text{mm})(0.651)\ 288]\}w_t$
   $= 0.226\ w_t$.
8. $K_f = 0.11 + [(0.226\ w_t - 0.11)(1 - 0.11)]/[0.226\ w_t - 2(0.11) + 1]$
   $= 0.11 + (0.226\ w_t - 0.11)(0.89)/(0.226\ w_t + 0.78)$.

9. At $H_f = n$, $w_{te} = 0.11/0.226 = 0.486$ mm.
10. $q_b = 373.4\ (w_t)^{0.67}$, where w_t is in millimeters and q_b is in kPa.
11. $Q_{te} = 11.69\ (0.226)(0.486)(288) + (0.2922)(373.4)(0.486)^{0.67}$ $Q_{te} = 370 + 67.3 = 437$ kN (Eq. 3.44).
12. $Q_{te} = 437$ kN, $w_{te} = 0.486$ mm is the point at the end of the linear portion of the load settlement curve.
13. Compute the values of Q_t for selected values of w_t on the nonlinear portion of the load-settlement curve. Numerical evaluations are made below.

Smooth Socket

w_t mm	H_f	$K_f =$	q_b kPa	Q_b kN	Q_s kN	Q_t kN
1	0.23	0.213	373	109.1	717	826
2	0.45	0.357	594	173.6	1203	1377
3	0.68	0.457	780	227.9	1539	1767
4	0.91	0.530	945	276.3	1785	2061
5	1.13	0.586	1098	320.8	1972	2293
6	1.36	0.630	1240	362.5	2120	2482
7	1.58	0.665	1375	402.0	2239	2641
8	1.81	0.694	1504	439.6	2337	2777
9	2.04	0.719	1628	475.7	2420	2896
10	2.26	0.740	1747	510.5	2491	3001
11	2.49	0.758	1862	544.1	2551	3095
12	2.72	0.773	1974	576.8	2604	3181
13	2.94	0.787	2082	608.6	2650	3259
14	3.17	0.799	2188	639.6	2691	3331
15	3.40	0.810	2292	669.8	2728	3398
16	3.62	0.820	2393	699.4	2761	3460
17	3.85	0.829	2492	728.4	2791	3519
18	4.08	0.837	2590	756.9	2817	3574
19	4.30	0.844	2685	784.8	2842	3627
20	4.53	0.851	2779	812.2	2864	3676
21	4.75	0.857	2872	839.2	2885	3724
22	4.98	0.862	2692	865.8	2904	3770
23	5.21	0.868	3052	891.9	2921	3813
24	5.43	0.873	3140	917.7	2937	3855
25	5.66	0.877	3227	943.2	2953	3896

14. The numerical values for a smooth socket are graphed in Figure 11.13 in comparison with the values from a rough socket to illustrate the effect of borehole roughness in this problem. Note again that $q_b < 2.5\ q_u$.

Side Resistance in Cohesive Intermediate Geomaterials—Uplift Loading Side resistance in uplift loading for cohesive intermediate geo-

materials is identical to that developed in compressive loading, provided that the shaft borehole is rough. If the shaft borehole is smooth, Poisson's effect reduces shaft resistance because the normal stress at the side of the borehole is reduced.

When the borehole is smooth, $f_{\max}$ should be reduced from the value computed for compressive loading by a factor Ψ:

$$f_{\max}\ (\text{uplift}) = \Psi\ f_{\max}\ (\text{compression}) \tag{11.50}$$

The value of Ψ is taken to be 1.0 when $(E_c/E_m)\ (B/D)^2 \geq 4$, or 0.7 when $(E_c/E_m)\ (B/D)^2 < 4$, unless field loading tests are performed. E_c and E_m are the composite Young's modulus of the shaft's cross section and rock mass, respectively, B is the socket diameter, and D is the socket length.

End Bearing in Cohesive Intermediate Geomaterials Several procedures are available for estimating the undrained unit end bearing in jointed rock. The procedures of Carter and Kulhawy (1988) and of the *Canadian Foundation Engineering Manual* (Canadian Geotechnical Society, 1992) are presented.

The method developed by Carter and Kulhawy (1988) can be used to estimate a lower bound for end bearing on randomly jointed rock. The same solution is used either for a shaft base bearing on the surface of the rock or for a base socketed into rock. It is assumed that

- the joints are drained,
- the rock between the joints is undrained,
- the shearing stresses in the rock mass are nonlinearly dependent on the normal stresses at failure,
- the joints are not necessarily oriented in a preferential direction,
- the joints may be open or closed, and
- the joints may be filled with weathered geomaterial (gouge).

End-bearing resistance is computed by

$$q_{\max} = \left(\sqrt{s} + \sqrt{m\sqrt{s} + s}\right) q_u \tag{11.51}$$

The parameters s and m for the cohesive intermediate geomaterial are roughly equivalent to c' and ϕ' for soil. The term in parentheses is analogous to the parameter N_c for clay soils. Values of s and m for cohesive intermediate geomaterial are obtained from Tables 11.8 and 11.9.

The second method for computing resistance in end bearing for drilled shafts in jointed, sedimentary rock, where the joints are primarily horizontal,

TABLE 11.8 Descriptions of Rock Types for Use in Table 11.9

Rock Type	Rock Description
A	Carbonate rocks with well-developed crystal cleavage (dolostone, limestone, marble)
B	Lithified argillaceous rocks (mudstone, siltstone, shale, slate)
C	Arenaceous rocks (sandstone, quartz)
D	Fine-grained igneous rocks (andesite, dolerite, diabase, rhyolite)
E	Coarse-grained igneous and metamorphic crystalline rocks (amphibolite, gabbro, gneiss, granite, norite, quartzdirorite)

is the method of the *Canadian Foundation Engineering Manual* (Canadian Geotechnical Society, 1992):

$$q_{\max} = 3K_{sp}\, d\, q_u \tag{11.52}$$

$$d = 1 + 0.4\,\frac{D_s}{B} \le 3.4 \tag{11.53}$$

$$K_{sp} = \frac{3 + c_s/B_b}{10\sqrt{1 + 300\,\delta/c_s}} \tag{11.54}$$

where

TABLE 11.9 Values of *s* and *m* Based on Rock Classification

Rock Quality	Joint Description and Spacing	Value of m as a Function of Rock Type (A–E) from Table 11.8					
		s	A	B	C	D	E
Excellent	Intact (closed); spacing <3 m	1	7	10	15	17	25
Very good	Interlocking spacing of 1 to 3 m	0.1	3.5	5	7.5	8.5	12.5
Good	Slightly weathered; spacing of 1 to 3 m	0.04	0.7	1	1.5	1.7	2.5
Fair	Moderately weathered; spacing of 0.3 to 1 m	10^{-4}	0.14	0.2	0.3	0.34	0.5
Poor	Weathered with gouge (soft material); spacing of 30 to 300 mm	10^{-5}	0.04	0.05	0.08	0.09	0.13
Very poor	Heavily weathered; spacing of less than 50 mm	0	0.007	0.01	0.015	0.017	0.025

q_{max} = unit end-bearing capacity,
K_{sp} = empirical coefficient that depends on the spacing of discontinuities,
q_u = average unconfined compressive strength of the rock cores,
c_s = spacing of discontinuities,
δ = thickness of individual discontinuities,
D_s = depth of the socket measured from the top of rock (not the ground surface), and
B_b = diameter of the socket.

The above equations are valid for a rock mass with spacing of discontinuities greater than 12 in. (0.3 m) and thickness of discontinuities less than 0.2 in. (5 mm) (or less than 1 in. [25 mm] if filled with soil or rock debris) and for a foundation with a width greater than 12 in. (305 mm). For sedimentary or foliated rocks, the strata must be level or nearly so. Note that Eq. 11.52 is different in form from that presented in the *Canadian Foundation Engineering Manual* in that a factor of 3 has been added to remove the implicit factor of safety of 3 contained in the original form. Further, note that the form of Eq. 11.53 differs from that in the first edition of the *Manual*.

11.6.5 Design for Axial Capacity in Cohesionless Intermediate Geomaterials

Cohesionless intermediate geomaterials are residual or transported materials that exhibit N_{60}-values of more than 50 blows per foot. It is common practice to treat these materials as undrained because they may contain enough fine-grained material to significantly lower permeability.

The following design equations are based on the original work of Mayne and Harris (1993) and modifications by O'Neill et al. (1996). The theory was proposed for gravelly soils, either transported or residual, with penetration resistances (from the SPT) between 50 and 100. The method has been used by Mayne and Harris to predict and verify the behavior of full-scale drilled shafts in residual micaceous sands from the Piedmont province in the eastern United States. Further verification tests were reported by O'Neill et al. for granular glacial till in the northeastern United States.

Side Resistance in Cohesionless Intermediate Geomaterial The maximum load transfer in side resistance in Layer i can be estimated from

$$f_{max,i} = \sigma'_{vi} K_{0i} \tan \phi'_i \tag{11.55}$$

where σ'_{vi} is the vertical effective stress at the middle of Layer i. The earth pressure coefficient K_{0i} and effective angle of internal friction of the gravel ϕ' can be estimated from field or laboratory testing or from

$$K_{0i} = (1 - \sin \phi_i')\left(\frac{0.2N_{60,i}}{\sigma_{vi}'/p_a}\right)^{\sin\phi_i'} \tag{11.56}$$

$$\phi_i' = \tan^{-1}\left\{\left[\frac{N_{60,i}}{12.2 + 20.3(\sigma_v'/p_a)}\right]^{0.34}\right\} \tag{11.57}$$

where $N_{60,i}$ is the SPT penetration resistance, in blows per foot (or blows per 300 mm), for the condition in which the energy transferred to the top of the drive string is 60% of the drop energy of the SPT hammer, uncorrected for the effects of overburden stress; and p_a is the atmospheric pressure in the selected system of units (usually 1 atmosphere, which converts to 101.4 kPa or 14.7 psi).

Side Resistance in Cohesionless Intermediate Geomaterial—Uplift Loading The equations for side resistance in uplift for cohesionless soils can be used for cohesionless intermediate geomaterials. The pertinent equations are Eqs. 11.23, 11.24, and 11.25.

End Bearing in Cohesionless Geomaterial Mayne and Harris (1993) developed the following expression for unit end-bearing capacity for cohesionless intermediate geomaterials:

$$q_{\max} = 0.59\left[N_{60}\left(\frac{p_a}{\sigma_{vb}'}\right)\right]^{0.8}\sigma_{vb}' \tag{11.58}$$

where N_{60} is the blow count immediately below the base of the shaft.

The value of $q_{\max}$ should be reduced when the diameter of the shaft B_b is more than 1.27 m (50 in.). If the diameter of the shaft is between 1.27 and 1.9 m (50 to 75 in.), $q_{\max,r}$ is computed using

$$q_{\max,r} = \frac{1.27}{B_b\ (\text{m})}\,q_{\max} \tag{11.59}$$

and if the shaft diameter is more than 1.9 m:

$$q_{\max,r} = q_{\max}\left[\frac{2.5}{aB_b\ (\text{m}) + 2.5b}\right] \tag{11.60}$$

where

$$a = 0.28B_b \text{ (m)} + 0.083 \frac{L}{B_b} \tag{11.61}$$

$$b = 0.065\sqrt{s_{ub} \text{ (kPa)}} \tag{11.62}$$

where

L = depth of base below the ground surface or the top of the bearing layer if the bearing layer is significantly stronger than the overlying soils, and

s_{ub} = average undrained shear strength of the soil or rock between the elevation of the base and $2B_b$ below the base. If the bearing layer is rock, s_{ub} can be taken as $q_u/2$.

The above equations are based on load tests of large-diameter underreamed drilled shafts in very stiff clay and soft clay-shale. These equations were developed assuming $q_{\max,r}$ to be the net bearing stress at a base settlement of 2.5 in. (64 mm) (O'Neill and Sheikh, 1985; Sheikh et al., 1985). When one-half or more of the design load is carried in end bearing and a global factor of safety is applied, the global factor of safety should not be less than 2.5, even if soil conditions are well defined, unless one or more site-specific load tests are performed.

Commentary on the Direct Load-Settlement Method This method is intended for use with relatively ductile weak rock, in which deformations occur in asperities prior to shear. If the weak rock is friable or unusually brittle, the method may be unconservative, and appropriate loading tests should be conducted to ascertain the behavior of the drilled shaft for design purposes. The method is also intended for use with drilled shafts in weak rocks produced in the dry. If it is necessary to produce the shaft using water, or with mineral or synthetic drilling slurries, the shaft should be treated as smooth for design purposes unless it can be proved that rough conditions apply. The method also assumes that the bearing surface at the base of the socket is clean, such that the shaft concrete is in contact with undisturbed weak rock. If base cleanliness cannot be verified during construction, base resistance (q_b) should be assumed to be zero.

The design examples did not consider the effect of a phreatic surface (water table) above the base of the socket. This effect can be handled by computing σ_n, assuming that the unit weight of the concrete below the phreatic surface is its buoyant unit weight:

$$\sigma_n = M[\gamma_c z_w + \gamma_c' (z_c - z_w)] \tag{11.63}$$

where

γ'_c = buoyant unit weight of concrete,
M is obtained from Figure 11.7, and
z_w = depth from top of concrete to elevation of water table.

11.6.6 Design for Axial Capacity in Massive Rock

Computation Procedures for Rock A broad view of the classification of intact rock can be obtained by referring to Figure 11.14 (Deere, 1968, and

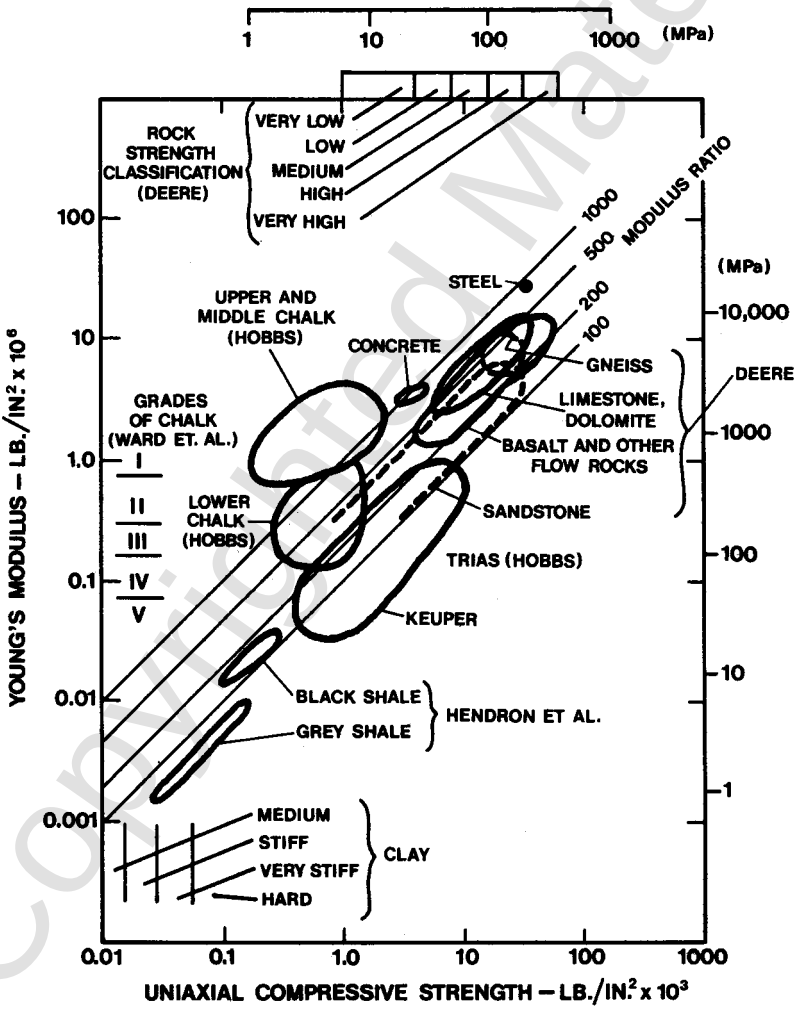

Figure 11.14 Engineering classification of intact rock (after Deere, 1968, by Horvath and Kenney, 1979).

Peck, 1976, as presented by Horvath and Kenney, 1979). The figure shows medium clay at the low range and gneiss at the high range. Concrete and steel are also shown for reference. Several of the rock categories have compressive strengths that are in the range of that for concrete or higher. As can be expected, many of the design procedures for drilled shafts in rock are directed at weak rock because strong rock could well be as strong as or stronger than the concrete in the drilled shaft. In this situation, the drilled shaft would fail structurally before any bearing capacity failure could occur.

Except for instances where drilled shafts were installed in weak rocks such as shales or mudstones, there are virtually no occasions where loading has resulted in failure of the drilled shaft foundation. An example of a field test where failure of the drilled shaft was impossible is shown in Figures 11.15 and 11.16. The rock at the site was a vuggy limestone that was difficult to core without fracture. Only after considerable trouble was it possible to obtain the strength of the rock. Two compression tests were performed in the laboratory, and in situ grout-plug tests were performed under the direction of Schmertmann (1977).

The following procedure was used for the in situ grout-plug tests. A hole was drilled into the limestone, followed by placement of a high-strength steel bar into the excavation, casting of a grout plug over the lower end of the bar, and pulling of the bar after the grout had cured. Five such tests were per-

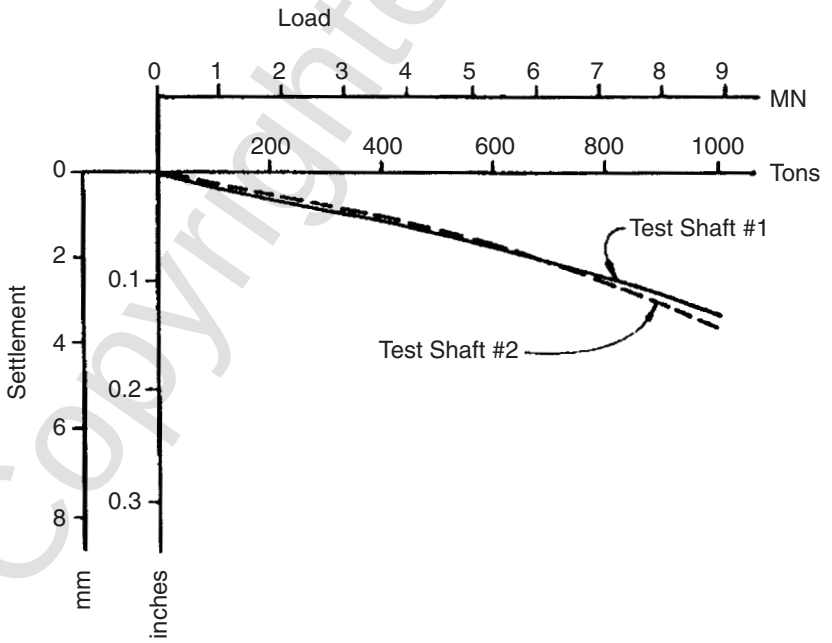

Figure 11.15 Load-settlement curves for Test Shafts No. 1 and 2, Florida Keys.

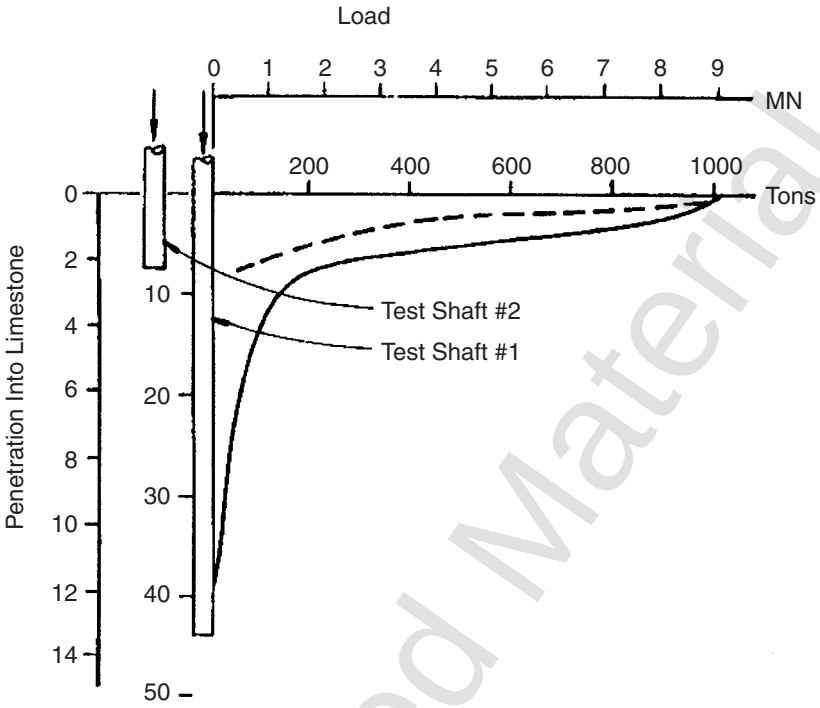

Figure 11.16 Load-distribution curves for Test Shafts Nos. 1 and 2, Florida Keys.

formed over the top 10 ft of the rock. Side resistance ranged from 12.0 to 23.8 tons/ft^2 (1.15 to 2.28 MPa), with an average of approximately 18.0 tons/ft^2 (1.72 MPa). The compressive strength of the rock was approximately 500 psi (3.45 MPa), putting the vuggy limestone in the lower ranges of the strength of the chalk shown in Figure 11.14.

Two axial load tests were performed at the site on cylindrical drilled shafts that were 36 in. (914 mm) in diameter (Reese and Nyman, 1978). Test Shaft No. 1 penetrated 43.7 ft (13.3 m) into the limestone, and Test Shaft No. 2 penetrated 7.6 ft (2.32 m). Test Shaft No. 1 was loaded first, with the results shown in Figures 11.15 and 11.16, and it was then decided to shorten the penetration and construct Test Shaft No. 2. As may be seen in Figure 11.15, the load-settlement curves for the two shafts are almost identical, with Test Shaft No. 2 showing slightly more settlement at the 1000-ton (8.9-MN) load (the limit of the loading system). The settlement of the two shafts under the maximum load is quite small, and most of the settlement (about 0.10 in., 2.5 mm) was due to elastic shortening of the drilled shafts.

The distribution of load with depth, determined from internal instrumentation in the drilled shafts, for the maximum load is shown in Figure 11.16. As may be seen, no load reached the base of Test Shaft No. 1, and only about

60 tons (530 kN) reached the base of Test Shaft No. 2. The data allowed a design for the foundations to be made at the site with confidence; however, as indicated, it was impossible to find the ultimate values of load transfer in side resistance and in end bearing because of the limitations of the loading equipment in relation to the strength of the rock. The results are typical for drilled shafts that are founded in rock that cannot develop the ultimate values of load transfer.

A special program of subsurface exploration is frequently necessary to obtain the in situ properties of the rock. Not only is it important to obtain the compressive strength and stiffness of the sound rock, but it is necessary to obtain detailed information on the nature and spacing of joints and cracks so that the stiffness of the rock mass can be determined. The properties of the rock mass will normally determine the amount of load that can be imposed on a rock-socketed drilled shaft. The pressuremeter has been used to investigate the character of in situ rock, and design methods have been proposed based on such results.

An example of the kind of detailed study that can be made concerns the mudstone of Melbourne, Australia. The Geomechanics Group of Monash University in Melbourne has written an excellent set of papers on drilled shafts that give recommendations in detail for subsurface investigations, determination of properties, design, and construction (Donald et al., 1980; Johnston et al., 1980a, 1980b; Williams, 1980; Williams et al., 1980a, 1980b; Williams and Erwin, 1980). These papers imply that the development of rational methods for the design of drilled shafts in a particular weak rock will require an extensive study and, even so, some questions may remain unanswered. It is clear, however, that a substantial expenditure for the development of design methods for a specific site could be warranted if there is to be a significant amount of construction at the site.

Williams et al. (1980b) discussed their design concept and stated: ''A satisfactory design cannot be arrived at without consideration of pile load tests, field and laboratory parameter determinations and theoretical analyses; initially elastic, but later hopefully also elastoplastic. With the present state of the art, and the major influence of field factors, particularly failure mechanisms and rock defects, a design method must be based primarily on the assessment of field tests.''

Other reports on drilled shafts in rock confirm the above statements about a computation method; therefore, the method presented here must be considered to be approximate. Detailed studies, including field tests, are often needed to confirm a design.

The procedure recommended by Kulhawy (1983) presents a logical approach. The basic steps are as follows.

1. The penetration of the drilled shaft into the rock for the given axial load is obtained by using an appropriate value of side resistance (see the later recommendation).

2. If the full load is taken by the base of the drilled shaft, the settlement of the drilled shaft in the rock is computed by adding the elastic shortening to the settlement required to develop end bearing. The stiffness of the rock mass is needed for this computation.
3. If the computed settlement is less than about 0.4 in. (10 mm), the side resistance will dominate and little load can be expected to reach the base of the foundation.
4. If the computed settlement is more than about 0.4 in. (10 mm), the bond in the socket may be broken and the tip resistance will be more important.

Kulhawy (1983) presents curves that will give the approximate distribution of the load for Steps 3 and 4; however, the procedure adopted here is to assume that the load is carried entirely in side resistance or in end bearing, depending on whether or not the computed settlement is less or more than 0.4 in.

The recommendations that follow are based on the concept that side resistance and end bearing will not develop simultaneously. The concept is conservative, of course, but it is supported by the fact that the maximum load transfer in side resistance in the rock will occur at the top of the rock, where the relative settlement between the drilled shaft and the rock is greatest. If the rock is brittle, which is a possibility, the bond at the top of the rock could fail, with the result that additional stress is transferred downward. There could then be a progressive failure in side resistance.

Note that the settlement will be small if the load is carried only in side resistance. The settlement in end bearing could be considerable and must be checked as an integral part of the analysis.

The following specific recommendations are made to implement the above general procedure:

1. Horvath and Kenney (1979) did an extensive study of the load transfer in side resistance for rock-socketed drilled shafts. The following equation is in reasonable agreement with the best-fit curve that was obtained where no unusual attempt was made to roughen the walls:

$$f_s \text{ (psi)} = 2.5\sqrt{q_u \text{ (psi)}} \tag{11.64}$$

where

f_s = ultimate side resistance in units of lb/in.^{2}, and
q_u = uniaxial compressive strength of the rock or concrete, whichever is less in units of lb/in^2.

(Note: Equation 11.61 is nonhomogeneous, and the value of q_u must be converted to English units, the equation solved for f_s in English units, and f_s

then converted to SI units before performing further computations with SI units.)

Note that there was a large amount of scatter in the data gathered by Horvath and Kenney (1979), but Eq. 11.64 can be used to compute the necessary length of the socket. If the drilled shaft is installed in clay-shale, the ultimate side resistance may be predicted more accurately by the procedures described in the previous section for clay-shale rather than by using Eq. 11.64.

2. The shortening ρ_c of the drilled shaft can be computed by elementary mechanics, employing the dimensions of the shaft and the stiffness of the concrete:

$$\rho_c = \frac{Q_{ST}L}{AE_c} \tag{11.65}$$

where

L = penetration of the socket,
Q_{ST} = load at the top of the socket,
A = cross-sectional area of the socket, and
E_c = equivalent Young's modulus of the concrete in the socket, considering the stiffening effects of any steel reinforcement.

3. The settlement of the base of the shaft can be obtained by assuming that the rock will behave elastically. The following equation will give an acceptable result:

$$w = \frac{Q_{ST}I_\rho}{B_bE_m} \tag{11.66}$$

where

w = settlement of the base of the drilled shaft,
I_ρ = influence coefficient,
B_b = diameter of drilled shaft, and
E_m = modulus of the in situ rock, taking the joints and their spacing into account.

4. The value of I_ρ can be found by using Figure 11.17. The symbol E_c in the figure refers to Young's modulus of the concrete in the drilled shaft. The value of Young's modulus of the intact rock E_L can be obtained by test or by selecting an appropriate value from Figure 11.14. The value of the modulus of the in situ rock can be found by test, or the intact modulus can be modified in an approximate way. Figure 11.18 allows modification of the modulus of

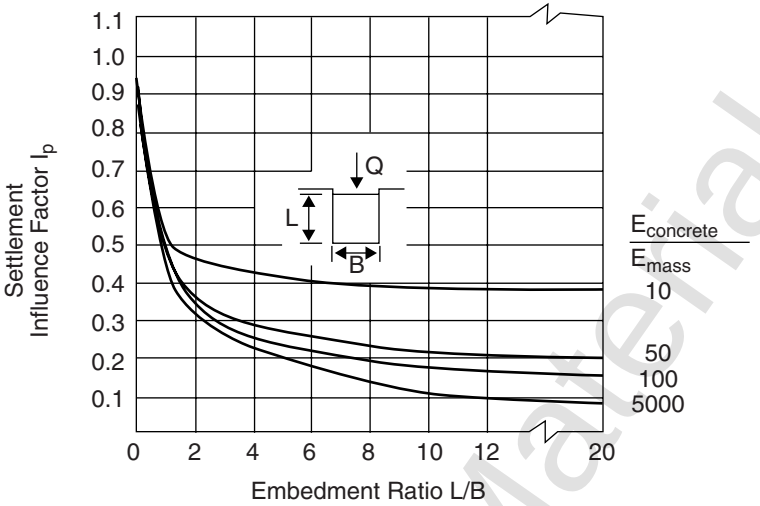

Figure 11.17 Elastic settlement influence factor as a function of embedment ratio and modular ratio (after Donald et al., 1980).

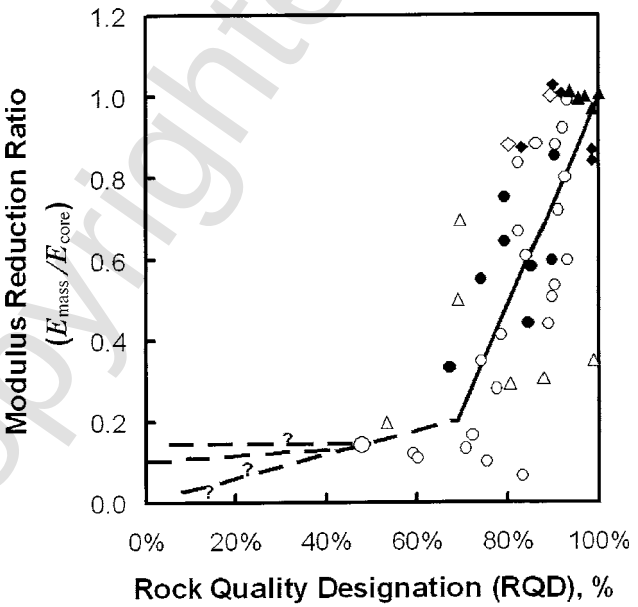

Figure 11.18 Modulus reduction ratio as a function of RQD (from Bieniawski, 1984).

the intact rock by using the RQD. As may be seen, the scatter in the data is great but the trend is unmistakable.

5. The bearing capacity of the rock can be computed by a method proposed by the Canadian Geotechnical Society (1978):

$$q_a = K_{sp}\, q_u \tag{11.67}$$

$$K_{sp} = \frac{3 + c_s/B_b}{10\sqrt{1 + 300\ \delta/c_s}} \tag{11.68}$$

where

q_a = allowable bearing pressure,
K_{sp} = empirical coefficient that depends on the spacing of discontinuities and includes a factor of safety of 3,
q_u = average unconfined compressive strength of the rock cores,
c_s = spacing of discontinuities,
δ = thickness of individual discontinuities, and
B_b = diameter of socket.

6. Equation 11.65 is valid for a rock mass with spacing of discontinuities greater than 12 in. (305 mm) and thickness of discontinuities less than 0.2 in. (5 mm) (or less than l in. [25 mm] if filled with soil or rock debris), and for a foundation with a width greater than 12 in. (305 mm). For sedimentary or foliated rocks, the strata must be level or nearly so (Canadian Geotechnical Society, 1978). Again, if the drilled shaft is seated on clay-shale, the procedures described in the previous section should provide a better prediction.

7. If the rock is weak (compressive strength of less than 1000 psi), the design should depend on load transfer in side resistance. The settlement should be checked to see that it does not exceed 0.4 in.

8. If the rock is strong, the design should be based on end bearing. The settlement under working load should be computed to see that it does not exceed the allowable value as dictated by the superstructure.

For the equations for the design of drilled shafts in rock to be valid, the construction must be carried out properly. Because the load-transfer values are higher for rock, the construction requires perhaps more attention than does construction in other materials. For example, for the load transfer in side resistance to attain the allowable values, there must be a good bond between the concrete and the natural rock. An excellent practice is to roughen the sides of the excavation if this appears necessary. There may be occasions when the drilling machine is underpowered and water is placed in the excavation to facilitate drilling. In such a case, the sides of the excavation may

be ''gun barrel'' slick, with a layer of weak material. Roughening of the sides of the excavation is imperative.

Any loose material at the bottom of the excavation should be removed even though the design is based on side resistance.

Another matter of concern with regard to construction in rock is whether or not the rock will react to the presence of water or drilling fluids. Some shales will lose strength rapidly in the presence of water.

Example Problem 5—Shaft in Rock This is an example of a drilled shaft into strong rock.

Soil Profile. The soil profile is shown in Figure 11.19. Only a small amount of water was encountered at the site during the geotechnical investigation.

Soil Properties. The dolomite rock found at the site had a compressive strength of 8000 psi, and the RQD was 100%. Young's modulus of the intact rock was estimated as 2.0×10^6 psi, and the modulus of the rock mass was identical to this value. Assume that the spacing of discontinuities is about 7 ft and that the thickness of the discontinuities is negligible.

Construction. The excavation can be made dry. A socket can be drilled into the strong rock and inspected carefully before concrete is poured.

Loading. The lateral load is negligible. The working axial load is 300 tons. No downdrag or uplift is expected.

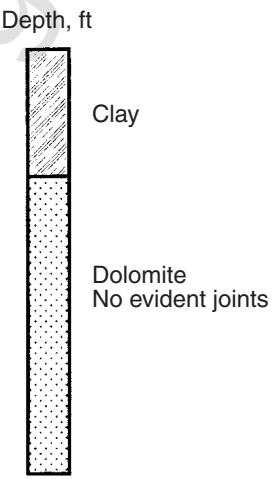

Figure 11.19 General soil and rock description of Example Problem 5.

Factor of Safety. An overall factor of safety of 3 is selected.

Geometry of the Drilled Shaft. A diameter of 3.5 ft is selected, and a socket of 3.5 ft into the dolomite is specified.

Hand Computations. Assuming that all load is transferred in end bearing and using the method proposed by the Canadian Geotechnical Society (1978):

$$q_a = K_{sp}\, q_u$$
$$q_a = (0.5)(8000) = 4000 \text{ psi}$$
$$Q_B = (4000)(\pi/4)(42)^2 = 5.54 \times 10^6 \text{ lb} = 2771 \text{ tons}$$

Note: The value of end bearing includes a factor of safety of 3.

11.6.7 Addition of Side Resistance and End Bearing in Rock

The decision to add or not to add side resistance and end bearing in rock must be made on a case-by-case basis using engineering judgment. A short discussion of several commonly encountered cases follows.

If only compression loading is applied and massive rock exists, it may only be necessary to penetrate the massive rock a short distance, large enough to expose the sound rock. In this situation, only end bearing is counted on because the distance of penetration (usually just a few inches) is too short for any significant side resistance to be developed.

In cases where a rock socket is formed to provide uplift resistance, the decision on whether to add side and base resistance for establishing the ultimate bearing capacity in compression is a matter of engineering judgment in which the nature of the rock must be considered. There are two possible cases. If the rock is brittle, it is possible that the majority of side resistance may be lost as settlement increases to the amount required to fully mobilize end bearing. It would not be reasonable to add side and base resistances together in this situation because they would not occur at large amounts of settlement. If the rock is ductile in shear and deflection softening does not occur, then side resistance and end bearing resistance can definitely be added together.

In cases where end bearing is questionable because of poor rock quality, the length of shafts is often extended in an effort to found the tip of the shaft in good-quality rock. In such situations, the rock socket may become long enough to develop substantial axial capacity in side resistance. In such situations, it is permissible to add side and base resistance together to obtain the total axial capacity of the shaft. Often, questions about the nature of the rock are best answered by conducting a well-planned load test on a full-size test shaft using an Osterberg load cell. The results of such a load test can establish the actual axial load capacity. If the actual axial capacity is sufficiently high,

the results of the load test may be used to reduce the size of the foundation shafts to obtain a more economically efficient design.

11.6.8 Commentary on Design for Axial Capacity in Karst

Design of drilled shaft foundations in karst presents the foundation designer with dangerous situations not found elsewhere. In karst geology, the depth to rock is uncertain (i.e., pinnacled rock), solution cavities may be present, numerous seams of softer materials may be present in the rock, and rock ledges and floaters may be encountered above the bearing strata.

These situations make it difficult for the designer to obtain accurate subsurface information from the field exploration program. The uncertain conditions caused by karst make it difficult for the designing engineer to prepare foundation plans and specifications. In such situations, it is mandatory that the engineer recognize the following:

- The field exploration must be more extensive than usual.
- Any change in structure location, or increased loading, will require existing field data to be reviewed and additional field exploration to be conducted to obtain the necessary information.
- Foundation plans and specifications should be written to anticipate the likely changed conditions to be encountered.
- It may be necessary to provide a means in the specifications to set the maximum length of drilled shafts based on side resistance alone when poor end-bearing conditions are encountered during construction.
- It is mandatory to prepare the plans and specifications in a manner consistent with existing purchasing regulations and in sufficient detail that each bid proposal will cover an identical scope of work.

The above conditions make it difficult to estimate the cost of construction accurately. In conditions with pinnacled rock, it may be necessary to drill additional exploratory borings at the location of every drilled shaft to obtain realistic estimates of foundation depths prior to the finalization of bid documents. In such situations, it is mandatory that the additional borings extend to depths greater than the planned depths of the foundations to ensure that no solution cavities exist below the foundations.

The issues discussed in the preceding paragraphs can only be resolved by a thorough field investigation. In some situations with karst, it will be necessary to conduct two or more phases of field boring programs to obtain the necessary information on which to base bid documents.

In large projects with highly variable conditions, use of *technique* shafts may be warranted prior to submission of bids for foundation construction. Technique shafts are full-sized demonstration shafts that are drilled on site. In this practice, all interested contractors are required to be on site to observe

the drilling of the technique shafts before they submit their bids for shaft construction. Observation of the technique shafts allows the interested contractors to observe the local conditions to determine the tools and equipment required to complete the job successfully. Use of technique shafts has reduced claims for changed conditions on many projects.

11.6.9 Comparison of Results from Theory and Experiment

Several studies have compared axial capacities computed using the static design methods to experimentally measured axial capacities. The results from one study by Isenhower and Long (1997) are presented in Figure 11.20. The data in this figure represent a database of axial load tests on drilled shafts that was compiled independently of the database used by Reese and O'Neill when developing the FHWA axial capacity methods.

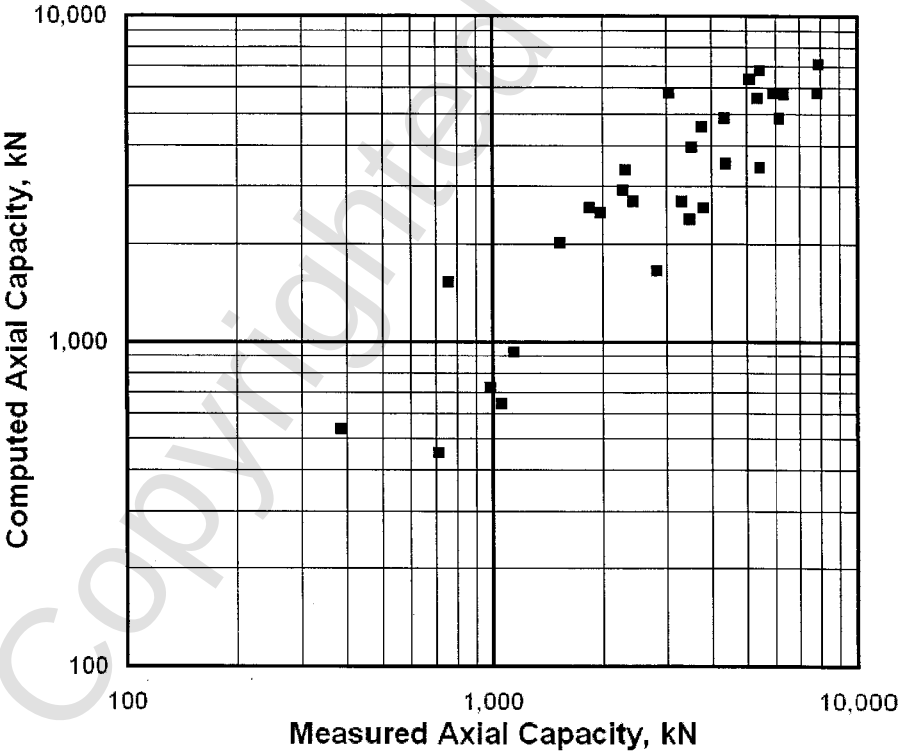

Figure 11.20 Computed axial capacity versus measured axial capacity (from Isenhower and Long, 1997).

PROBLEMS

P11.1. Compute the axial capacity of drilled sand in sand. The shaft diameter is 3 ft and the length is 50 ft.

The soil profile is:

0–20 ft, average N_{60} = 11 blows/ft, γ = 115 pcf
20–50 ft, average N_{60} = 32 blows/ft, γ = 120 pcf
50–80 ft, average N_{60} = 35 blows/ft, γ = 123 pcf

The depth of the water table is 10 ft.

P11.2. What is the allowable axial capacity of the foundation in P11.1 if a factor of safety of 3 is used?

P11.3. Develop a bearing graph for the shaft of P11.1. Plot axial capacity on the horizontal axis and shaft length on the vertical axis. Include shaft lengths from 10 ft to 50 ft, at 5 ft intervals.

P11.4. Develop a bearing graph for shafts in the soil profile of P11.1 for shaft diameters of 2, 3, 4, 5, 6, 7, and 8 ft. Include shaft lengths from 10 ft to 50 ft, at 5 ft intervals.

P11.5. Using the bearing graph of P11.4, estimate the cost of the shaft dimensions that would have allowable capacities of 100 tons, using a factor of safety of 3 and unit cost figures provided by your instructor.

P11.6. Consider a deep layer of sand extending from the ground surface to a depth of 40 meters. For this sand, γ = 18 kN/m^3 and the water table is at the ground surface. Calculate the axial capacity in side resistance for a shaft with a 1 m diameter and a length of 32 m. Perform the computations using a single layer, two equally thick layers, and four equally thick layers. How does the thickness of the layer affect the computed results?

P11.7. Compute the axial capacity of a drilled shaft in a cohesive soil profile. The shaft diameter is 4 ft and the length is 65 ft.

The soil profile is:

0–15 ft, c = 2200 psf, γ = 120 pcf
15–30 ft, c = 2700 psf, γ = 123 pcf
30–55 ft, c = 3250 psf, γ = 125 pcf
55–100 ft, c linearly varying with depth from 3250 to 4400 psf, γ = 130 pcf

The depth of the water table was 15 ft.

P11.8. What is the axial uplift capacity of the shaft of P11.7.

P11.9. Compute the axial capacity of the drilled shaft of P11.7 with a 3-m, 45 deg. Bell.

P11.10. What are the exclusion zones from side resistance for compression loading for the shaft of P11.7?

P11.11. What are the exclusion zones from side resistance for uplift loading for the shaft of P11.7?

P11.12. What are the exclusion zones from side resistance for compression loading for the shaft of P11.9?

P11.13. What are the exclusion zones from side resistance for uplift loading for the shaft of P11.9?

P11.14. Compute the axial capacity of a rock socket. The rock joints are horizontal and closed. The uniaxial compressive strength is 12 MPa, and the RQD = 75%. The diameter of the socket is 1 m and the depth is 3.5 m. Show the computations for side resistance and base resistance.

P11.15. Discuss the situations when axial side resistance and end bearing can be combined for rock sockets and when they cannot be combined.